International Journal of Nanomedicine

Dovepress
open access to scientific and medical research

Open Access Full Text Article

ORIGINAL RESEARCH

Fatty Oil of Descurainia Sophia Nanoparticles Improve Monocrotaline-Induced Pulmonary Hypertension in Rats Through PLC/IP3R/Ca^{2+} Signaling Pathway

Yajuan Zheng[1,*], Peipei Yuan[1,2,*], Zhenkai Zhang[1], Yang Fu[1,2], Saifei Li[1], Yuan Ruan[1], Panying Li[1], Yi Chen[1], Weisheng Feng[1–3], Xiaoke Zheng[1–3]

[1]College of Pharmacy, Henan University of Chinese Medicine, Zhengzhou, 450008, People's Republic of China; [2]The Engineering and Technology Center for Chinese Medicine Development of Henan Province, Zhengzhou, 450046, People's Republic of China; [3]Collaborative Innovation Center for Chinese Medicine and Respiratory Diseases Co-Constructed by Henan province & Education Ministry of P. R. China, Zhengzhou, 450008, People's Republic of China

*These authors contributed equally to this work

Correspondence: Weisheng Feng; Xiaoke Zheng, Email fwsh@hactcm.edu.cn; zhengxk.2006@163.com

International Journal of Nanomedicine downloaded from https://www.dovepress.com/
For personal use only.

Purpose: Fatty oil of *Descurainia Sophia* (OIL) has poor stability and low solubility, which limits its pharmacological effects. We hypothesized that fatty oil nanoparticles (OIL-NPs) could overcome this limitation. The protective effect of OIL-NPs against monocrotaline-induced lung injury in rats was studied.

Methods: We prepared OIL-NPs by wrapping fatty oil with polylactic-polyglycolide nanoparticles (PLGA-NPs) and conducted in vivo and in vitro experiments to explore its anti-pulmonary hypertension (PH) effect. In vitro, we induced malignant proliferation of pulmonary artery smooth muscle cells (RPASMC) using anoxic chambers, and studied the effects of OIL-NPs on the malignant proliferation of RPASMC cells and phospholipase C (PLC)/inositol triphosphate receptor (IP3R)/Ca^{2+} signal pathways. In vivo, we used small animal echocardiography, flow cytometry, immunohistochemistry, western blotting (WB), polymerase chain reaction (PCR) and metabolomics to explore the effects of OIL-NPs on the heart and lung pathological damage and PLC/IP3R/Ca^{2+} signal pathway of pulmonary hypertension rats.

Results: We prepared fatty into OIL-NPs. In vitro, OIL-NPs could improve the mitochondrial function and inhibit the malignant proliferation of RPASMC cells by inhibiting the PLC/IP3R/Ca^{2+}signal pathway. In vivo, OIL-NPs could reduce the pulmonary artery pressure of rats and alleviate the pathological injury and inflammatory reaction of heart and lung by inhibiting the PLC/IP3R/Ca^{2+} signal pathway.

Conclusion: OIL-NPs have anti-pulmonary hypertension effect, and the mechanism may be related to the inhibition of PLC/IP3R/Ca^{2+}signal pathway.

Keywords: pulmonary hypertension, PLC/IP3R/Ca^{2+}, nanoparticles, RPASMC, fatty oil

Introduction

Pulmonary hypertension (PH) is a pulmonary vascular disease characterized by progressive elevation of pulmonary artery pressure. In severe cases, right heart failure or even death may occur.[1] The survey showed that the incidence rate and mortality of PH increase year by year.[2,3] PH is a refractory disease that seriously threatens human health, and its pathogenesis is complex and the result of the interaction of many factors.[4] Pulmonary artery pressure is mainly affected by pulmonary blood flow and pulmonary vascular resistance. Any structural and functional abnormality that leads to an increase in pulmonary artery blood flow and pulmonary artery resistance can cause an increase in pulmonary artery pressure. Studies have shown that pulmonary hypertension is mainly caused by genetics, drugs and various heart and lung diseases.[5] In the pathological state of pulmonary hypertension, the stimulation of inflammation, hypoxia and other factors leads to the organic and functional lesions of pulmonary

Received: 20 September 2023
Accepted: 20 November 2023
Published: 8 December 2023

© 2023 Zheng et al. This work is published and licensed by Dove Medical Press Limited. The full terms of this license are available at https://www.dovepress.com/terms.php and incorporate the Creative Commons Attribution – Non Commercial (unported, v3.0) License (http://creativecommons.org/licenses/by-nc/3.0/). By accessing the work you hereby accept the Terms. Non-commercial uses of the work are permitted without any further permission from Dove Medical Press Limited, provided the work is properly attributed. For permission for commercial use of this work, please see paragraphs 4.2 and 5 of our Terms (https://www.dovepress.com/terms.php).

Graphical Abstract

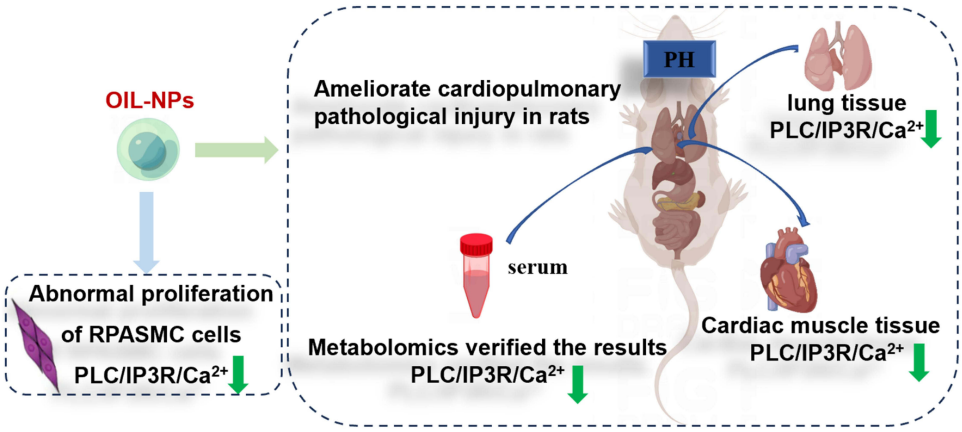

arterioles, and then the function of endothelial cells is impaired. The secretion of a variety of vasoactive substances involved in endothelial cell function becomes unbalanced. This leads to excessive proliferation of smooth muscle cells in the media of the pulmonary arteries and lumen occlusion, resulting in an increase in pulmonary artery pressure. Long-term elevated pulmonary artery pressure leads to increased right heart workload and even right heart failure.[6]

The main pathological changes of pulmonary hypertension include pulmonary vasoconstriction, pulmonary remodeling and in situ thrombosis.[7,8] Studies have shown that inhibition of malignant proliferation of arterial smooth muscle cells can effectively improve pulmonary vascular remodeling, thereby alleviating the symptoms of pulmonary hypertension.[9,10] Further studies have shown that the increase in intracellular Ca^{2+} concentration may be at core of the development of pulmonary hypertension. Intracellular Ca^{2+} overload promotes pulmonary vascular immune inflammatory response, pulmonary vascular endothelial cell dysfunction, pulmonary vascular remodeling, right heart dysfunction and other pathological changes in the process of pulmonary hypertension.[11–13] Similarly, it has been shown that elevated cytosolic Ca^{2+} concentration stimulates abnormal proliferation of PASMCs.[14] PLC is a key enzyme that promotes phosphatidylinositol metabolism and calcium signaling. PLC/IP3R pathway is a classical Ca^{2+} signaling pathway.[15] Studies have shown that in PASMC of patients with pulmonary hypertension, the PLC/IP3R calcium signaling pathway promotes the increase in cytosolic Ca^{2+} concentration in PASMC, and then promotes the proliferation of pulmonary artery smooth muscle cells.[12,16] Therefore, the excessive activation of PLC/IP3R/Ca^{2+} signaling pathway is closely related to the abnormal proliferation of PASMC cells.[17]

In recent years, traditional Chinese medicine has received extensive attention due to its significant efficacy and safety. *Descurainia sophia* (known as Tinglizi in Chinese) is a traditional herb of the Brassicaceae family that is mainly used in Northeast Asia, including Korea, Japan, and China, to treat lung diseases.[18] Previous studies have shown that *Descurainia sophia* can reduce pulmonary inflammation, inhibit lung cancer cell proliferation, and attenuate myocardial injury and cardiac remodeling.[19–21] Our laboratory has previously conducted a systematic study on *Descurainia sophia*, and found that *Descurainia sophia* has good effects in treating lung diseases[22] and improving pulmonary hypertension, and can significantly inhibit the expression of PLC.[23] According to the types and polarity of *Descurainia sophia*, the fractions were divided into five fractions: fatty oil, oligosaccharides, flavonoid glycosides, flavonoid aglycones, and polysaccharides. Further studies found that the fatty oil fractions had good activity, but their anti-PH effects were not clear.[19] Therefore, the present experiment investigated whether fatty oil could exert its anti-pH effect by inhibiting PLC/IP3R/Ca^{2+} signaling pathway.

GC-MS analysis revealed that the main component in fatty oil is 9, 12-octadecadienoic acid, 10,13,16-docosatrienoate, linolenic acid, etc. Studies have shown that these fatty acids have good effects on inhibiting tumor cells, regulating immune inflammation and protecting lung parenchyma.[21,24,25] In addition, the combination of fatty acids can better regulate the balance of fatty acids in the body, thereby improving the disease.[26,27] However, these fatty acids are poorly water soluble and their double bonds are easily oxidized. The preparation of drugs into appropriate nano preparations can

improve the solubility of drugs, improve the bioavailability of drugs, and increase the efficacy.[28,29] Therefore, we prepared OIL-NPs and conducted and in vitro experiments to explore their anti-PH effects.

Materials and Methods

Chemicals

Descurainia sophia was purchased from Tongrentang Drugstore in Beijing (Zhengdong New Area Store). Preparation of the fatty oil component of the seed of *Descurainia sophia*: After the seed of *Descurainia sophia* is powdered, it is extracted with a certain amount of petroleum ether, and then concentrated and dried under reduced pressure to obtain the fatty oil component. The extraction rate of fatty oil was 28.8%.[19]

Study on Composition of Fatty Oil

The composition of fatty oil was analyzed by Gas Chromatography-Mass Spectrometer (GC-MS), and the process was as follows: 4 mL n-hexane was added to fatty oil (about 100 mg), followed by 1 mL 0.8 mol/L NaOH methanol solution, and vortex for 5 min, dried with 0.5 g $NaHSO_4$, centrifuged for 10 min, then supernatant was extracted, and dricated with 0.22 μm filter membrane, to be analyzed by GC-MS. The chromatographic conditions were as follows: a DB-5 quartz capillary column with high purity helium as carrier gas and helium flow rate of 1.0 mL/min. The inlet temperature was 280°C. Shunt injection, shunt ratio 10:1, injection volume 0.1 μL; The heating procedure is 50°C, keep for 2 min, then temperature rises to 200°C at 3°C/min, temperature rises to 300°C at 20°C/min, keep for 5 min, gasification chamber temperature 280°C, interface temperature 280°C. Mass spectrum conditions: collision gas velocity, helium 2.25 mL/min; nitrogen 1.5 mL/min; ion source: electron bombardment source, electron energy 70eV; scanning range 45–400 amu, ion source temperature 230°C, GC-MS interface temperature 280°C.

Preparation of OIL-NPs

The amount of fatty oil was weighed and diluted with PLGA solution (50 mg/mL, dichloromethane as solvent) to 5 mg/mL. They were dispersed into 1% PVA (PVA; MW = 30–70 kDa; HD, 80%) aqueous solution at a volume ratio of 1:5 and then phacoemulsified. A suspension of OIL-NPs was obtained after stirring the emulsion for 12 h to volatilize the dichloromethane. At room temperature, remove large particles by centrifuging with 2000×g for 2 min, and then centrifuging with 6000×g for 5 min to obtain precipitation. Wash with water twice to remove the unsealed drugs and impurities.

Evaluation of OIL-NPs Encapsulation Efficiency

After derivatization of linolenic acid reference, fatty oil samples, and OIL-NPs, drug loading and encapsulation efficiency were determined by HPLC. The HPLC conditions: C_{18} column, 244 nm UV detector, mobile phase: methanol: water = 93.5:6.5, column temperature 35°C, and flow rate 0.9 mL/min.

Characterization Studies of OIL-NPs

The polydispersity index (PDI), particle size distribution and particle size stability of OIL-NPs were measured by Zetasizer (Nano-ZS ZEN 3600; Malvern Instruments, Malvern, UK). The particle size morphology was observed by transmission electron microscopy.[30] OIL-NPs and fat-free NPs were prepared, freeze-dried, and analyzed by infrared spectroscopy to determine the structure of OIL-NPs (Nicolet iS 50; Thermo, USA). The small animal in vivo imaging system was used to detect the distribution of OIL-NPs in vivo. Cy7 (PC0020; Beijing Solarbio Science & Technology) were dissolved with PLGA (contains fatty oils) and emulsified with 1% PVA to form fluorescent drug-loaded nanoparticles. Male C57BL/N mice were injected with nanoparticles (5 $mg \cdot kg^{-1}$, calculated according to the concentration of Cy7) through the tail vein. At 3, 12 and 24 h after administration, the mice were anesthetized with isoflurane, and the fluorescence intensity of lung tissue was detected by small animal in vivo fluorescence imaging system (Pearl™ Imager, LI-COR, USA) and statistical analysis was performed.

In vitro Method

Cell Culture

RPASMC cells were purchased from Creative Bioarray. Cells were cultured in high-glucose medium (10% fetal bovine serum, 1% penicillin-streptomycin) at 37°C and 5% CO_2.

Determination of Apoptosis, Mitochondrial Levels and Cell Viability

In the in vitro experiment, normal group (NC), model group (M), fatty oil group (oil), fatty oil nanoparticle group (OIL-PLGA) and PLC agonist group (PLC+) were set up. The OIL group was given 100 μg/mL fatty oil, and the OIL-PLGA group was given with 100 μg/mL fatty oil-loaded PLGA nanoparticles, PLC+ group was given 5μmol/l PLC agonist (m-3M3FBS) (MCE company, HY-19619, Shanghai, China) and 100 μg/mL fatty oil-loaded PLGA nanoparticles. RPASMC cells were seeded in 96-well plates (2×10^4/ mL) or 6-well plates (4×10^4/mL). Except NC group, other groups were placed in a hypoxia chamber for 72 hours to establish the model. Cell viability was detected by CCK-8 assay (Abcam, Cambridge, UK). After the cells were treated with apoptosis kit (BD Biosciences, Franklin Lakes, NJ, USA), mitochondrial membrane potential detection kit and Ca^{2+} detection kit (Beyotime Biotechnology, Shanghai, China), the apoptosis rate, mitochondrial membrane potential change and intracellular Ca^{2+} content were detected by flow cytometry (BD Biosciences, Franklin Lakes, NJ, USA).[22]

In vivo Method

Establishment of an Animal Model

Six-week-old Specific Pathogen Free grade SD male rats, weighing 180–200 g (animal number: SCXK Beijing 2019-0008), were purchased from Beijing Huafukang Biotechnology Co., Ltd (Beijing China). SPF male C57BL/6N mice, aged 6–8 weeks, weighing 19–22 g, were purchased from Beijing Weitong Lihua Experimental Technology Co., LTD., license number: SCXK (Beijing) 2021–0006. Experimental animals were kept in a clean animal laboratory (18–20°C) with free access to food and water. Animal experiments were approved by Henan University of Traditional Chinese Medicine (Zhengzhou, China) (Ethics No. DWLL201908112). Experiments were carried out according to the guidelines and regulations of the Animal Care and Use Committee of the National Organization Engineering Center (Zhengzhou, China).

After a week of adaptive feeding, the animals were randomly divided into normal group (NC), model group (M), fatty oil low-dose group (OIL-L), fatty oil high-dose group (OIL-H), fatty oil nanoparticles low-dose group (OIL-PLGA-L), fatty oil nanoparticles high-dose group (OIL-PLGA-H), positive drug nifedipine group (NI) (MCE company, HY-B0284, Shanghai, China), PLC inhibitor neomycin sulfate group (PLC-) (MCE company, HY-B0470, Shanghai, China). Except NC group, the other groups were intraperitoneally injected with monocrotaline (60 mg/kg, i.p.) (MCE company, HY-N0750, Shanghai, China) on the first day to establish the model (pulmonary hypertension developed at 28 days).[31] Treatment was administered by injection (i.v.) on days 14 to 28 (every 2 days), with the following doses in each group: OIL-L (20 mg/kg), OIL-H (40 mg/kg), OIL-PLGA-L (20 mg/kg fatty oil-loaded PLGA nanoparticles), OIL-PLGA-H (40 mg/kg fatty oil-loaded PLGA nanoparticles), NI (0.1 mg/kg), PLC- (20 mg/kg).

Measurement of Pulmonary Artery Pressure and Right Heart Function

Pulmonary artery pressure and right heart function were measured by ultrasound imaging in small animals (VisualSonics, Toronto, Canada). After anesthesia, the rats were placed on the detection plate. Use the ultrasonic probe to closely fit the place where the coupling agent is applied in the rat's precordial region, and then twist the probe to find the appropriate section. M-ultrasound and Doppler ultrasound were used to measure the values, and then the results were analyzed.

Histological Assessment

Lung tissue and heart tissue were taken, fixed, paraffin embedded and sectioned. HE sections were obtained after staining with hematoxylin and eosin; Weigert's iron hematoxylin, acid fuchsin solution, and 1% phosphomolybdic acid aqueous solution were used to prepare Masson staining sections. Observe the pathological damage under the microscope and use ImagePro Plus 6.0 to save the picture.

Enzyme-Linked Immunosorbent Assay (ELISA)

The levels of brain natriuretic peptide (BNP) (MM-0067R1, Meimian, Jiangsu, China), endothelin-1 (ET-1) (MM-0560R1, Meimian, Jiangsu, China) and tumor necrosis factor-α (TNF-α) (MM-0180R1, Meimian, Jiangsu, China) in serum were detected by enzyme-linked immunosorbent assay (ELISA).

Measurement of NO in Serum

We used the NO detection kit to detect the NO content in rat serum (Jiancheng, Nanjing, China), and all operations were performed according to the instructions.

Western Blotting

Take the heart and lung tissue of rats, extract the protein according to the operating instructions of the protein extraction kit, and determine the protein concentration by BCA method. After determining the loading amount according to the protein concentration, the protein was separated by polyacrylamide gel electrophoresis. Proteins were transferred to PVDF membranes using the semi-dry method. After blocking PVDF membranes with 5% BSA for 1 h, PLC (1:1000, 19962-1-AP, Protentech), IP3R (1:1000, 66668-1-Ig, Protentech), STIM1 (1:1000, 11565-1-AP, Protentech), ORAI1 (1:1000, 28411-1-AP, Protentech), NF-κB (1:1000, 66535-1-Ig, Protentech), and β-actin (1:5000, 66009-1-Ig, Protentech) were added and incubated overnight at 4°C. After washing five times with 0.1% PBST, secondary antibody was added. Then, blots were washed thrice with 0.1% PBST. Odyssey two-color imaging system and Image Studio software were used for quantitative analysis of protein bands.

Real-Time RT-qPCR

Take the heart and lung tissue or pulmonary artery smooth muscle cells and extract the RNA according to the instructions of the total RNA extraction kit (Beijing Solarbio Science & Technology). After the RNA concentration of the samples was determined with an ultramicrospectrophotometer, the samples were put into a thermal cycler and reverse transcribed to obtain cDNA. The synthesized cDNA was amplified by real-time PCR. The probes for genes, including PLC, IP3R, STIM1, ORAI1, P65, Dynamin-related protein 1 (Drp1), mitofusin 2 (MFN2), TNF-α, interleukin-6 (IL-6), BCL2-Associated X (BAX), interleukin-1β (IL-1β), B cell lymphoma-2 (Bcl-2) and Caspase-3 were purchased from Beijing Genomics Institute (BGI). Reaction conditions: 25°C, 5 min; 42°C for 60 min; 80°C for 10 min; It was maintained at 4°C to obtain cDNA. The amplification was performed by fluorescence quantitative PCR instrument under the reaction conditions of 95°C and 10 s. 95°C, 5 s; 60°C, 10 s; A total of 40 cycles were performed. The amplification curve was analyzed and the Ct value was calculated. GAPDH was used as the reference gene, and the $2^{-\Delta\Delta Ct}$ method was used to calculate the relative expression of the target gene.[22] The sequences for the primers used in our study are listed in Table 1.

UPLC-Q-TOF-MS Analysis

About 100 μL of serum was mixed with 500 μL of cold acetonitrile, vortexed for 60 s, and centrifuged at 12,000 rpm for 10 min. After centrifugation, the supernatant was taken, diluted twice with distilled water, vortexed and centrifuged to obtain the tested samples. Serum samples were separated in a UHPLC system (AcclaimTMRSLC120 C18 (100 mm × 2.1 mm, 2.2 μm)). Column temperature: 40°C; Mobile phase: pure acetonitrile (A) and 0.1% formic acid aqueous solution (B); Flow rate: 0.3 mL/min; Injection volume: 2 μL. Gradient elution procedure: 0–6 min, 10–70% A; 6–14 min, 70–80% A; 14–16 min, 80–90% A. After preliminary separation of samples, the samples were analyzed by Q/TOF-MS equipped with electric spray ion source (ESI). Full scan quality data range: 50~1500 Da; Scanning time: 0.2 s; Desolvent gas flow rate: 8 L/min; Ion source energy: 3.0 eV; Capillary voltage: 3.5 kV (positive ion mode), 3.2 kV (negative ion mode); Calibration solution: sodium formate; Flow rate: 42 μL/h.[32]

Statistical Analyses

SPSS 20.0 statistical software was used for data analysis. Measurement data were expressed as mean ± standard deviation (x±s); One-way analysis of variance (one-way ANOVA) was used for comparison among multiple groups. $P < 0.05$ was considered statistically significant.

Table 1 Primer Sequences

Target	Forward Primer (5′-3′)	Reverse Primer (3′-5′)	Product Size
PLC	ATCCAGGAGGTGGTGCAGTA	ATCTGCAGCTTGGGCTTCTC	125
IP3R	GTTTTGTGGGAAACCGAGGC	CCAAGCATGCAAACCAAGA	104
STIM1	AGCTGCGTGACGAGATCAAT	TTTTGGCGGCTCCTCTCATT	91
ORAI1	CCGTTCACTTCTACCGCTCA	GCCCGGTGTTAGAGAATGGT	131
P65	TGTATTTCACGGGACCTGGC	CAGGCTAGGGTCAGCGTATG	110
Drp1	TTCTTCCCAGAGGGACTGGT	TCAACTCCATTTTCTTCTCCTGT	109
MFN2	CCCTCGACAGTGTTTCTCCC	CGGCTATTCTTAGGGCCCAG	138
TNF-α	CATCAAGAGCCCTTGCCCTA	CTGGAAGACTCCTCCCAGGTA	88
IL-6	GACTTCCAGCCAGTTGCCTT	AAGTCTCCTCTCCGGACTTGT	83
IL-1β	AGGCTGACAGACCCCAAAA	CTCCACGGGCAAGACATAGG	178
Bax	GACAGGGGCCTTTTTGCTAC	CACTCGCTCAGCTTCTTGGT	123
Bcl-2	GGTGAACTGGGGGAGGATG	AGAGCGATGTTGTCCACCAG	102
Caspase-3	GCTGGACTGCGGTATTGAGA	TAACCGGGTGCGGTAGAGTA	108
GAPDH	ACAGCAACAGGGTGGTGGC	TTTGAGGGTGCAGCGAACTT	252

Results

Analysis of Fatty Oil by GC-MS

Our laboratory had previously isolated and identified 64 components in fatty oil by gas chromatography-mass spectrometry (GC-MS) analysis, and 51 major components were identified by mass spectrum library search and retention index double qualitative method. The total relative content accounted for 97.75% of the total detected compounds. The substance with the most abundant content is 9.12-Octadecanedioic acid, methyl ester, accounting for 21.58%, followed by metal 10,13,16-docosatrienoate (19.39%). Linolenic acid, methyl ester (15.87%).[33] The total ion current is plotted in Figure 1. Since the fatty oil were methyl esterified before entering the GC-MS analysis, the GC-MS results showed that most of them were lipids. Therefore, most of the components in fatty oils are fatty acids. Studies have shown that unsaturated fatty acids such as Octadecanediynoic acid, docosatrienoate and Linolenic acid have good effects on inhibiting immune inflammatory response, inhibiting tumor cell proliferation, anti-asthma and regulating immune response.[25,34,35] Polyunsaturated fatty acids are tissue selective, and their combination can more comprehensively regulate the body's metabolic disorders, and exert specific metabolic effects under specific physiological and pathological conditions.[36–38]

Figure 1 Total ion current diagram of fatty oil.

Characterization of OIL-NPs

The experimental results show that linolenic acid standard substance was detected in about 10 min (Figure 2A). The chromatographic peaks of linolenic acid also appeared in the corresponding time of the chromatograms of fatty oil and OIL-NPs (Figure 2B and C). This indicates that the specificity of the experimental method is good. Taking the concentration (ug/mL) as the abscissa and the peak area as the ordinate, the linear regression equation of linolenic acid was y = 0.0083193X + 0.005803917000 (r = 0.9995). The results showed that the linearity of linolenic acid injection was good in the range of 1ug/mL-500ug/mL. According to the same method, the average recovery rate of fatty oil was 86.12%, RSD was 0.14%, and the recovery rate of OIL-NPs was 100.07%, RSD was 0.52%, which showed that the experimental method had good recovery and high accuracy.

Finally, the drug loading and encapsulation rate of OIL-NPs were measured as 5.30% ± 0.049% and 60.09% ± 0.55% by the above method.

The average particle size of the nanoparticles (NPs) without fat OIL was 137.9 ± 2.45nm (Figure 2D), and that of OIL-NPs was 323.87 ± 4.81 nm, and PDI was 0.157 ± 0.009 (Figure 2E), which indicated that the fatty oil was encapsulated in the nanoparticles, so the average particle size of OIL-NPs was larger. The average particle size of OIL-NPs was similar to that of PLGA drug-loaded nanoparticles reported in literature.[39,40] Moreover, the particle size of the OIL-NPs was determined for 7 consecutive days, and the results showed that the OIL-NPs had a good stability (Figure 2G). Transmission electron microscopy results showed that the nanoparticles were complete spherical particles, evenly dispersed among particles, and the particle size distribution was relatively uniform (Figure 2F).

In the OIL-NPs infrared spectrum, the C-H stretching vibration peak (3007 cm^{-1}, 2923 cm^{-1}, 2853 cm^{-1}), C-O-C stretching vibration peak (1160 cm^{-1}), and C-H bending vibration peak (718 cm^{-1}) of fatty oil (OIL) appeared. At the same time, it also contains the characteristic absorption peak of NPs, such as C=O stretching vibration peak (1747 cm^{-1}), C-H bending vibration (1449 cm^{-1}, 1383 cm^{-1}), C-O stretching vibration (1269 cm^{-1}), C-O-C stretching vibration (1086 cm^{-1}), C-H bending vibration peak (868 cm^{-1}). It can be seen that the infrared characteristic peaks of fatty oil and NPs simultaneously appear in the OIL-NPs spectrum, and a new C-O-C peak appears at 1130 cm^{-1}, which indicates that fatty oil and nanoparticles form a new ester absorption peak through chemical reaction (Figure 2H). This suggests the successful construction of OIL-NPs nanoparticles. In vivo imaging of small animals showed that OIL-NPs had accumulated in the lung tissue of mice 3 h after administration and could accumulate and stay in the lung tissue within 12 h and 24 h after administration (Figure 2I).

Effects of OIL-NPs on Hypoxic-Induced Abnormal Proliferation of RPASMC Cells

PH is closely related to the malignant proliferation of RPASMC cells. In vitro experiments were performed to investigate the effect of OIL-NPs on RPASMC cell proliferation. Seventy-two-hour hypoxia significantly promoted the proliferation of RPASMC cells (Figure 3A). We found that concentrations of 50μg/mL and above of fatty oil could significantly inhibit the proliferation of RPASMC cells (Figure 3B). Our previous studies have shown that the total extract of *Descurainia sophia* can inhibit PLC expression. In order to investigate whether fatty oil of *Descurainia Sophia* nanoparticles can inhibit PLC, we designed a PLC agonist group. 5 μM PLC agonist could significantly increase the expression level of PLC ($P<0.01$) (Figure 3C). The cell proliferation activity in group M was increased ($P<0.01$), the apoptosis rate was decreased ($P<0.01$), the mRNA levels of apoptosis-related indicators Bax and Caspase-3 were decreased ($P<0.01$), and the level of Bcl-2 was increased ($P<0.01$). OIL group and OIL-PLGA group can improve these indicators (Figure 3D–F). Moreover, the Ca^{2+} content, mitochondrial membrane potential and the mRNA levels of STIM1, ORAI1 and DRP1 in the OIL group and OIL-PLGA group were increased ($P<0.01$), while the mRNA level of MFN2 was decreased ($P<0.01$) (Figure 3G–I). However, there was no significant difference in PLC+ group. This indicates that the effect of OIL-NPs was weakened or disappeared after the addition of PLC inhibitors. These results suggest that OIL-NPs may inhibit the malignant proliferation of RPASMC cells by regulating the expression of PLC.

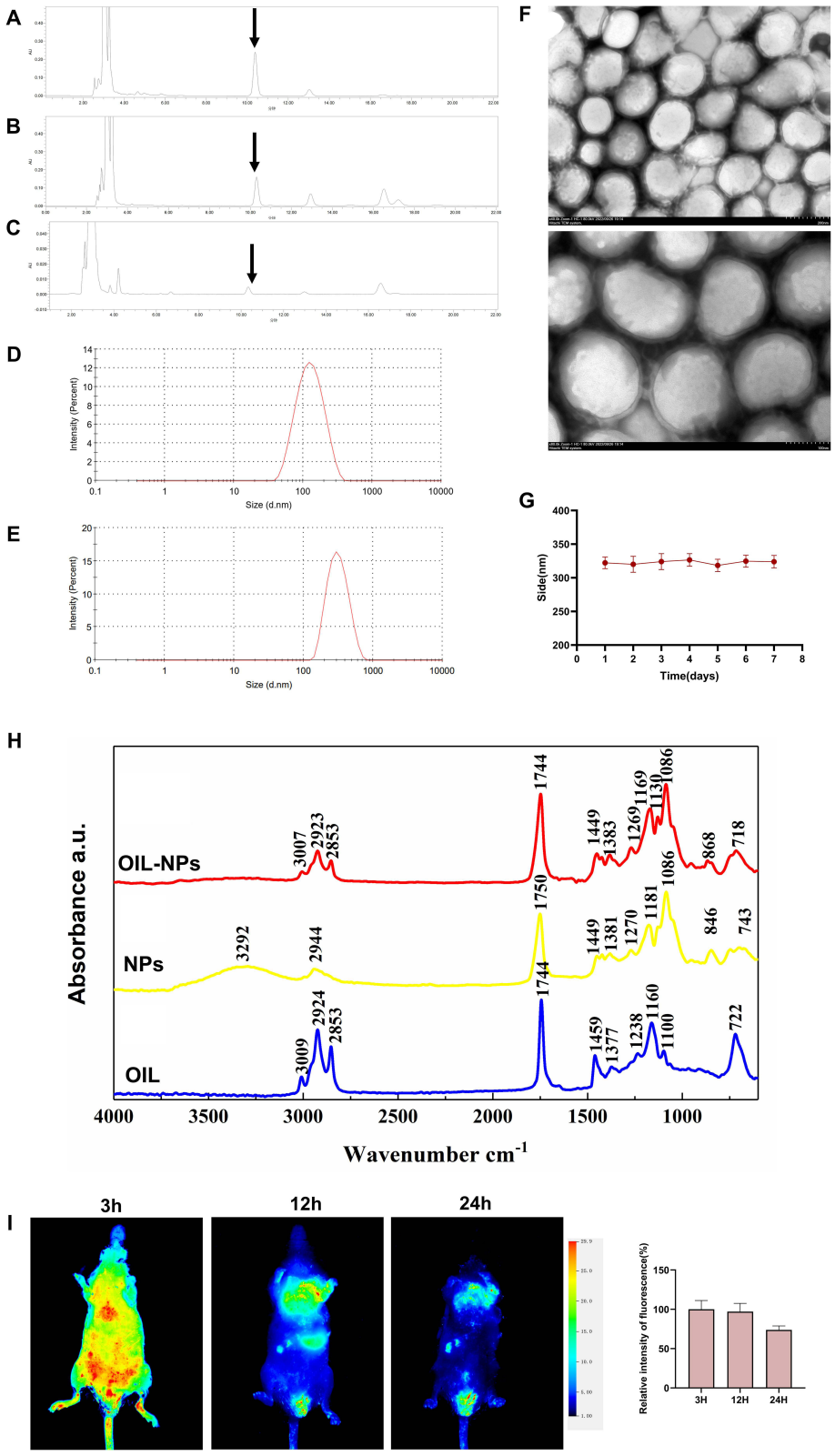

Figure 2 OIL-NPs of characterization(**A**) Chromatogram of linolenic acid. (**B**) Chromatogram of fatty oil. (**C**) Chromatogram of OIL-NPs (**D**) Mean particle size of nanoparticles (without fatty oil) (**E**) Average particle size of OIL-NPs. (**F**) OIL-NPs transmission electron microscope. (**G**) Particle size stability of OIL-NPs. (**H**) Fatty oil (OIL) (blue), nanoparticles (NPs) (yellow), fatty oil nanoparticles infrared absorption peak (OIL-NPs) (red) (**I**) in vivo distribution and targeting of OIL-NPs.

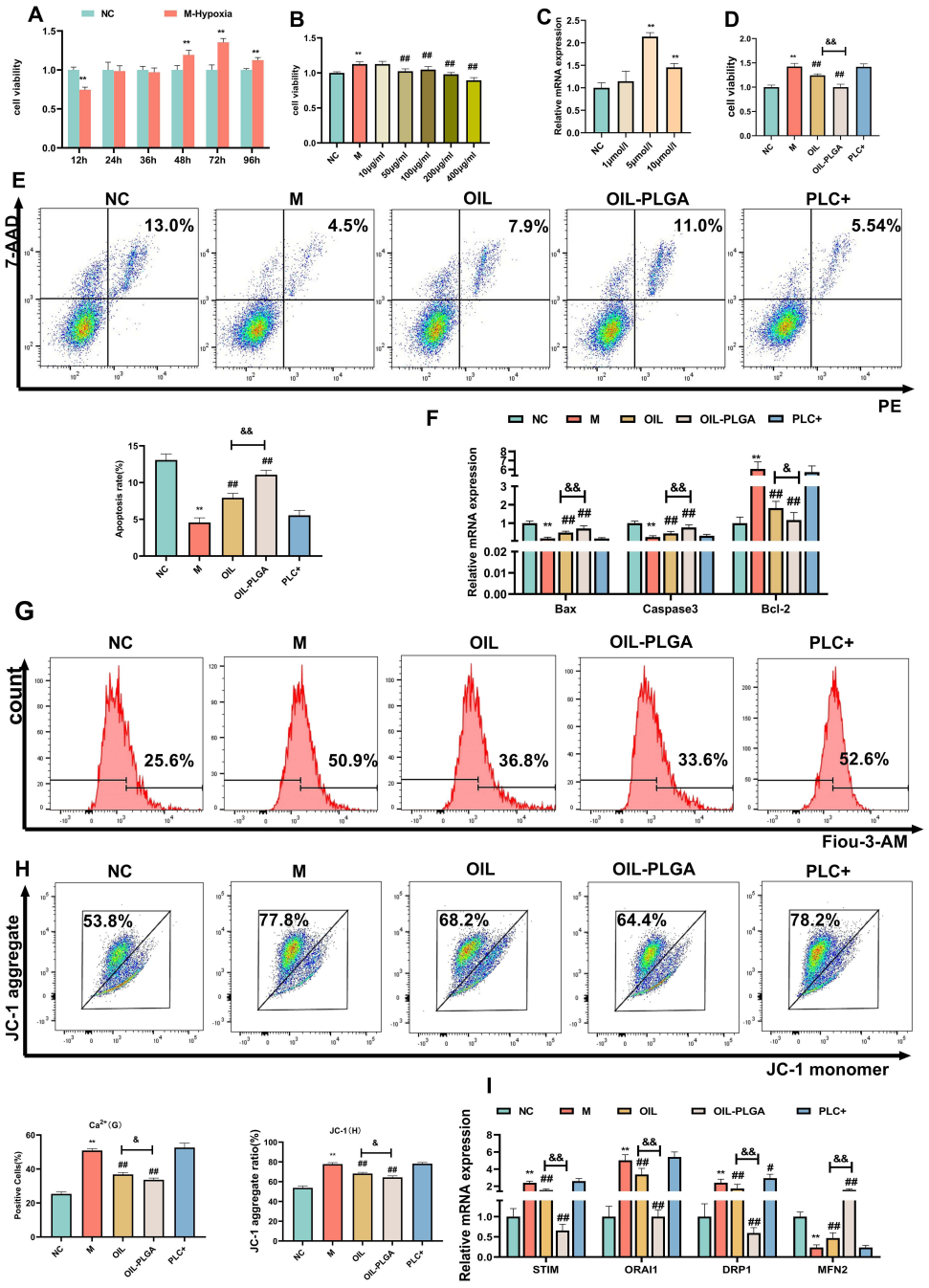

Figure 3 Effects of OIL-NPs on apoptosis and PLC/IP3R/Ca^{2+} signaling pathway in RPASMC cells. (**A**) Screening of RPASMC cells model; (**B**) Effect of different concentrations of fatty oil on cell viability of RPASMC. (**C**) Screening of optimal dose of PLC agonist. (**D**) Effect of OIL-NPs on RPASMC cells viability. (**E**) Effect of OIL-NPs on apoptosis of RPASMC cells. (**F**) Effect of OIL-NPs on mRNA expression levels of Bax, Bcl-2, and Caspase-3 in RPASMC cells. (**G**) Effect of OIL-NPs on Ca^{2+} content in RPASMC cells. (**H**) Effects of OIL-NPs on mitochondrial membrane potential in RPASMC cells. (**I**) Effects of OIL-NPs on STIM1, ORAI1, DRP1 and MFN2 mRNA expression levels in RPASMC cells.

Notes: Data are the mean ± SD (n = 6). $^{**}P<0.01$ vs the NC group. $^{\#\#}P<0.01$ vs the M group. $^{\&}P<0.05$, $^{\&\&}P<0.01$ vs the OIL group.

Abbreviations: NC, control group underwent standard culture; M, model group with hypoxic for 72 h; OIL, 50 μg/mL fatty oil, OIL-PLGA, 50 μg/mL fatty oil-loaded PLGA nanoparticles, PLC+, 5 μM m-3M3FBSd and 50 μg/mL fatty oil-loaded PLGA nanoparticles. Bax, BCL2-Associated X; Bcl-2, B cell lymphoma-2. Caspase-3, cysteine aspartic acid-specific protease 3. STIM1, stromal interaction molecule 1. ORAI1, calcium release-activated calcium channel modulator 1. Drp1, Dynamin-related protein 1. MFN2, mitofusin 2.

Effects of OIL-NPs on Pulmonary Artery Pressure and Right Heart Function in PH Rats

Weight is a key indicator for evaluating drug side effects. In this study, OIL-NPs did not affect the body weight of rats (Figure 4A). HE section and Masson staining of lung tissue showed that the wall of pulmonary vessels in group M was

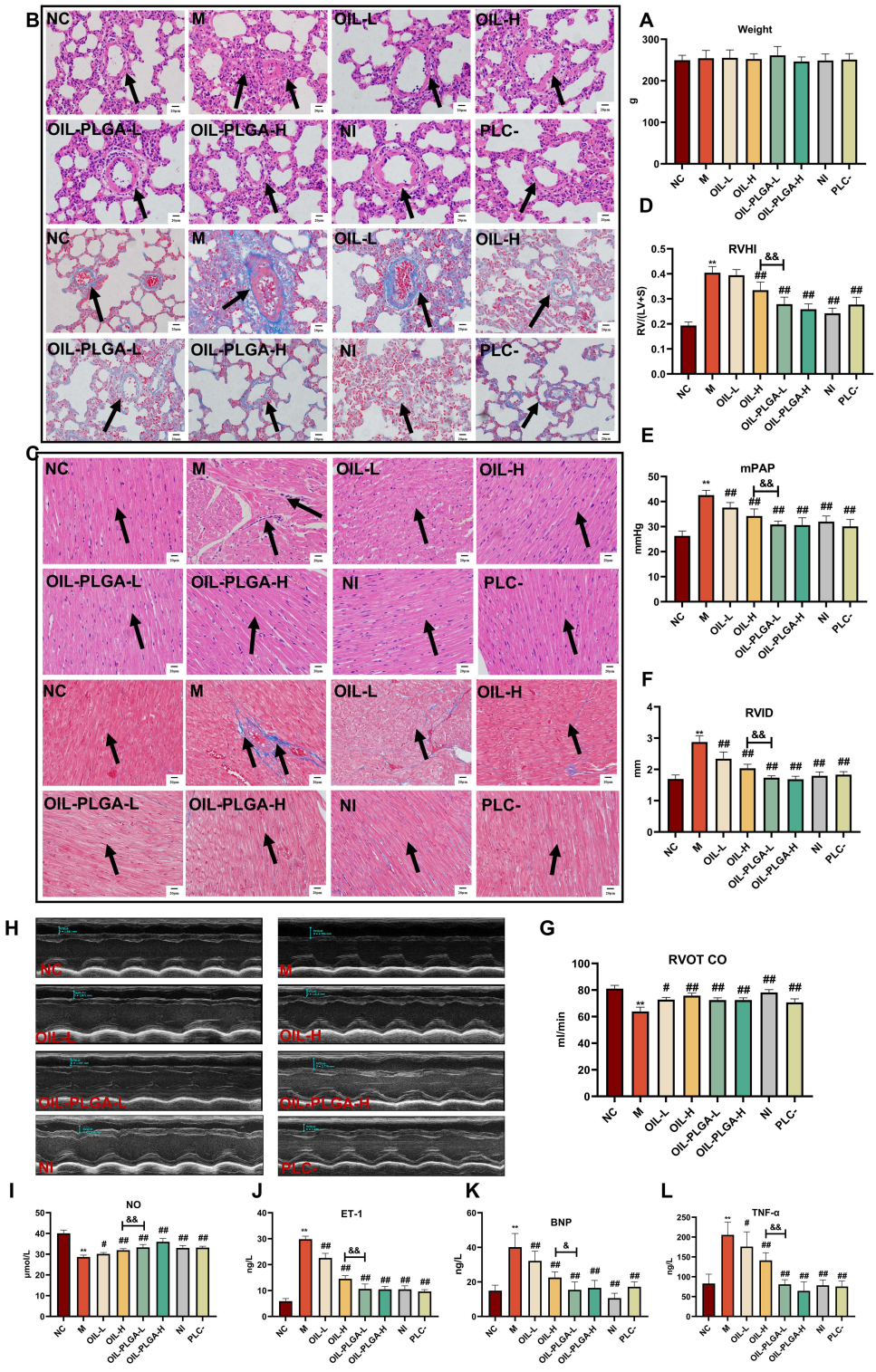

Figure 4 Effects of OIL-NPs on pathological injury of heart and lung and right heart function in PH rats; (**A**) Effects of OIL-NPs on weight in PH rats. (**B**) Effects of OIL-NPs on pathological injury of lung in PH rats (HE and Masson staining, ×400) (Black arrows point to the pulmonary vascular portion). (**C**) The effect of OIL-NPs on the pathological damage of myocardial tissue in PH rats (HE and Masson staining, ×400). (Black arrows point to disarranged, scarred, or neat portions of myocardial tissue) (**D**–**G**) Effects of OIL-NPs on pulmonary artery pressure and right ventricular function in PH rats. (**H**) Echocardiography of rats in each group. (**I**–**L**) Effects of OIL-NPs on the contents of NO, ET-1, BNP and TNF-α in serum of PH rats.

Notes: Data are the mean ± SD (n = 6). $^{**}P<0.01$ vs the NC group. $^{\#}P<0.05$, $^{\#\#}P<0.01$ vs the M group. $^{\&}P<0.05$, $^{\&\&}P<0.01$ vs the OIL-H group.

Abbreviations: NC, control group. M, model group with 60 mg/kg monocrotaline, i.p. OIL-L, 20 mg/kg fatty oil, i.v. OIL-H, 40 mg/kg fatty oil, i.v.; OIL-PLGA-L, 20 mg/kg fatty oil-loaded PLGA nanoparticles, i.v. OIL-PLGA-H, 40 mg/kg fatty oil-loaded PLGA nanoparticles, i.v. NI, 0.1 mg/kg nifedipine, i.v. PLC-, 20 mg/kg neomycin sulfate, i.v. RVHI, right ventricular hypertrophy index. mPAP, pulmonary artery pressure. RVID, inner diameter of right heart. RVOT CO, right cardiac output. ET-1, endothelin-1; TNF-α, tumor necrosis factor-α. BNP, brain natriuretic peptide; NO, nitric oxide.

thickened, collagen fibers were aggregated around pulmonary vessels, lumen was narrowed, and inflammatory cells were aggregated and infiltrated. The thickening of pulmonary vascular wall and the aggregation of collagen fibers were reduced in each treatment group (Figure 4B). HE section and Masson staining of myocardial tissue showed that there was no obvious necrosis and inflammatory cell infiltration between cells in each administration group, and the deposition of collagen fibers in the interstitial tissue of cardiac tissue was significantly reduced (Figure 4C).

Compared with the NC group, the right ventricular hypertrophy index (RVHI), pulmonary artery pressure (mPAP), inner diameter of right heart (RVID) in the M group were increased ($P<0.01$), and the right cardiac output (RVOT CO) in the M group was decreased ($P<0.01$). The above indexes were improved in different dosage groups ($P<0.01$ or $P<0.05$) (Figure 4D–H). The serum levels of ET-1, TNF-α and BNP in the model group were increased (P<0.01), and the serum level of NO was decreased (P<0.01). The serum levels of ET-1, TNF-α and BNP in the M group were increased ($P<0.01$), and the level of NO in the M group was decreased ($P<0.01$). Compared with the M group, the treatment groups showed improvement effect ($P<0.01$ or $P<0.05$) (Figure 4I–4L). In the above experimental results, the effect of OIL-PLGA-L group was stronger than that of OIL-H group ($P<0.01$ or $P<0.05$). These results suggested that fatty oil and OIL-NPs can reduce the pathological damage of heart and lung in PH rats, reduce pulmonary artery pressure, improve right heart function, and reduce the expression of inflammatory factors. According to the above results, the effect of OIL-H group was stronger than that of OIL-L group, while the effect of the OIL-PLGA-L was better than that of the OIL-H group. Therefore, the OIL-H group and the OIL-PLGA-L group were selected later for further mechanism exploration.

Effect of OIL-NPs on PLC/IP3R/Ca^{2+} Signaling Pathway in Lung Tissue of PH Rats

Compared with NC group, the protein and mRNA expressions of PLC, mRNA expressions of IP3R and Ca^{2+} content in lung tissue of M group were increased ($P<0.01$). The above indexes were decreased in each administration group ($P<0.01$) (Figure 5A–C). These results suggested that fatty oil and OIL-NPs may play an anti-pH role through the PLC/IP3R/Ca^{2+} signaling pathway. The protein expression of STIM1, ORAI1 and NF-κB was closely related to Ca^{2+} content. Our results show that the protein expression of STIM1, ORAI1 and NF-κB in lung tissue of M group was increased ($P<0.01$). Compared with M group, the protein expressions of STIM1, ORAI1 and NF-κB in the lung tissues of the rats in each treatment group were decreased ($P<0.01$) (Figure 5A). The mRNA expression of P65, TNF-α, IL-1β and IL-6 in lung tissue of rats in M group was increased ($P<0.01$). The mRNA levels of the above inflammatory factors could be decreased in each administration group ($P<0.01$) (Figure 5D). In the above experimental results, the effect of OIL-PLGA-L group was stronger than that of OIL-H group ($P<0.01$ or $P<0.05$). This further suggests that fatty oil and OIL-NPs may regulate Ca^{2+} through the PLC/IP3R/Ca^{2+} signaling pathway to reduce inflammatory response and thus play a role in anti-PH.

Effect of OIL-NPs on PLC/IP3R/Ca^{2+} Signaling Pathway in Myocardial Tissue of PH Rats

Compared with NC group, the protein and mRNA expression of PLC, IP3R mRNA expression and Ca^{2+} content in myocardial tissue of rats in M group were increased ($P<0.01$). The above indexes were decreased in each administration group ($P<0.01$) (Figure 6A–C). Similar to the results in lung tissue, the protein expression levels of STIM1, ORAI1, and NF-κB and the mRNA expression levels of TNF-α, IL-1β, IL-6, and P65 were reduced in each administration group ($P<0.01$ or $P<0.05$) (Figure 6D and E). In the above experimental results, the effect of OIL-PLGA-L group was stronger than that of OIL-H group ($P<0.01$ or $P<0.05$). These results suggest that OIL-NPs may play an anti-PH role through the PLC/IP3R/Ca^{2+} signaling pathway.

Metabolic Serum Profiling

The basal peak chromatogram of serum samples from rats was obviously separated, and evenly distributed, and the peak height of each group was different. The results showed that the metabolite content of M group and NC group and M group and OIL-PLGA-L group were changed (Figure 7A). In the PCA score plot, NC and M groups were separated, and the administration group and NC group were clustered into one group (Figure 7B), indicating that OIL-NPs had a good

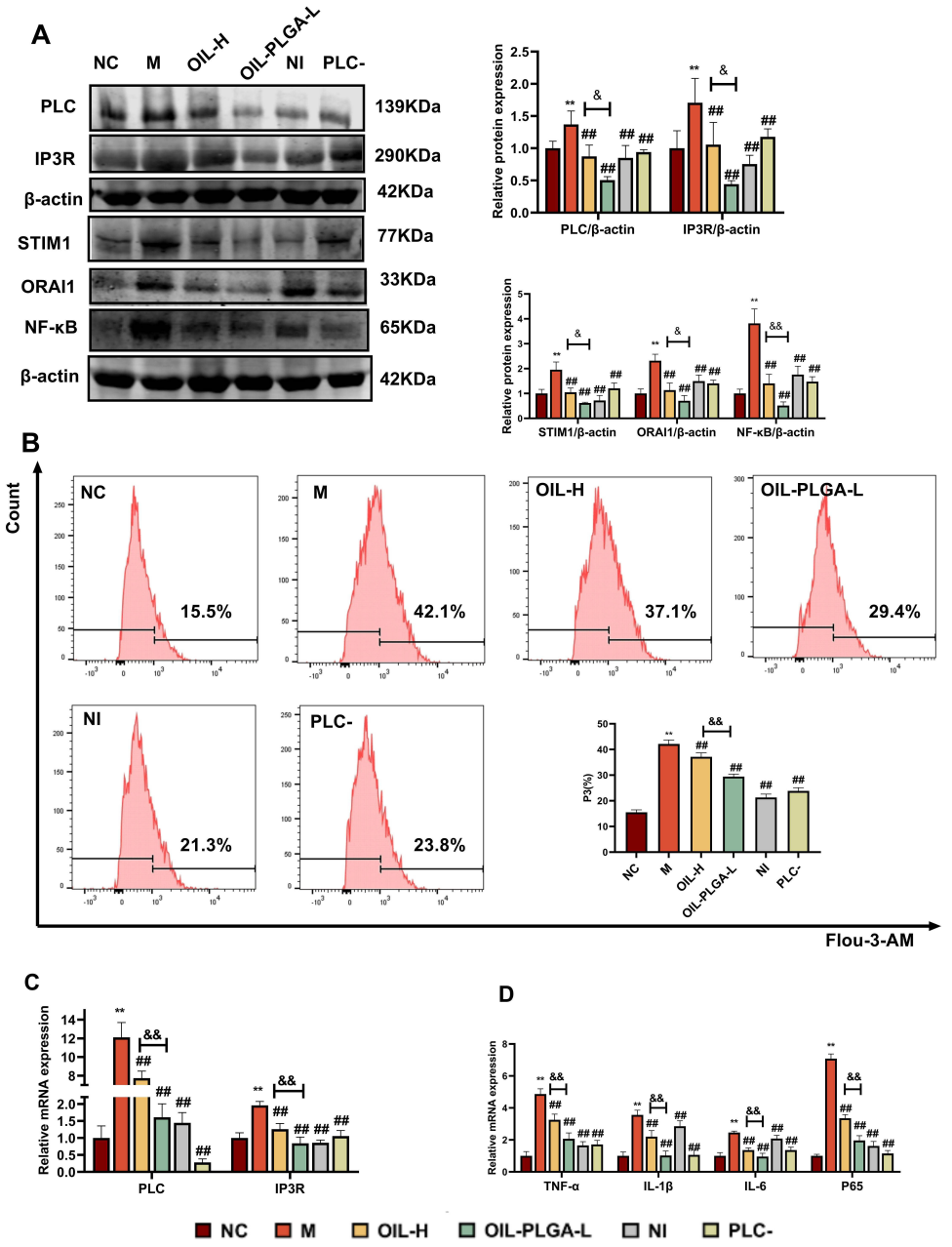

Figure 5 Effects of OIL-NPs on PLC/IP3R/Ca^{2+} signaling pathway in lung tissues of PH rats. (**A**) Effects of OIL-NPs on the expression of PLC/IP3R/Ca^{2+} related proteins in lung tissues of PH rats. (**B**) Effects of OIL-NPs on Ca^{2+} content in lung tissues of PH rats. (**C**) The effect of OIL-NPs on the expression of PLC and IP3R mRNA in the lung tissue of PH rats. (**D**) The effect of OIL-NPs on the mRNA expression levels of TNF-α, IL-1β, IL-6 and P65 in the lung tissue of PH rats.

Notes: Data are the mean ± SD (n = 6). $^{**}P<0.01$ vs the NC group. $^{\#\#}P<0.01$ vs the M group. $^{\&}P<0.05$, $^{\&\&}P<0.01$ vs the OIL-H group.

Abbreviations: NC, control group. M, model group with 60 mg/kg monocrotaline, i.p. OIL-H, 40 mg/kg fatty oil, i.v. OIL-PLGA-L, 20 mg/kg fatty oil-loaded PLGA nanoparticles, i.v. NI, 0.1 mg/kg nifedipine, i.v. PLC-, 20 mg/kg neomycin sulfate, i.v. PLC, primary antibodies against phospholipase C. IP3R, inositol 1,4,5-triphosphate receptor. STIM1, stromal interaction molecule 1. ORAI1, calcium release-activated calcium channel modulator 1. NF-κB, nuclear factor kappaB. TNF-α, tumor necrosis factor-α. IL-1β, interleukin-1β. IL-6, interleukin-6.

intervention effect on rats with pulmonary hypertension. In order to find the endogenous products that caused the metabolic profile changes in rats, OPLS-DA analysis was performed on the NC group, M group and OIL-PLGA-L group. The results showed that the NC group was significantly separated from the M group, and the M group was separated from the OIL-PLGA-L group (Figure 7C–F). S-plot analysis was performed on OPLS-DA score maps, and biomarkers with large differences were selected according to VIP>3 and $P<0.05$. Finally, a total of 50 biomarkers were identified, there were 24 identical markers in NC group, M group and OIL-PLGA-L group (including 15 positive source markers and 9

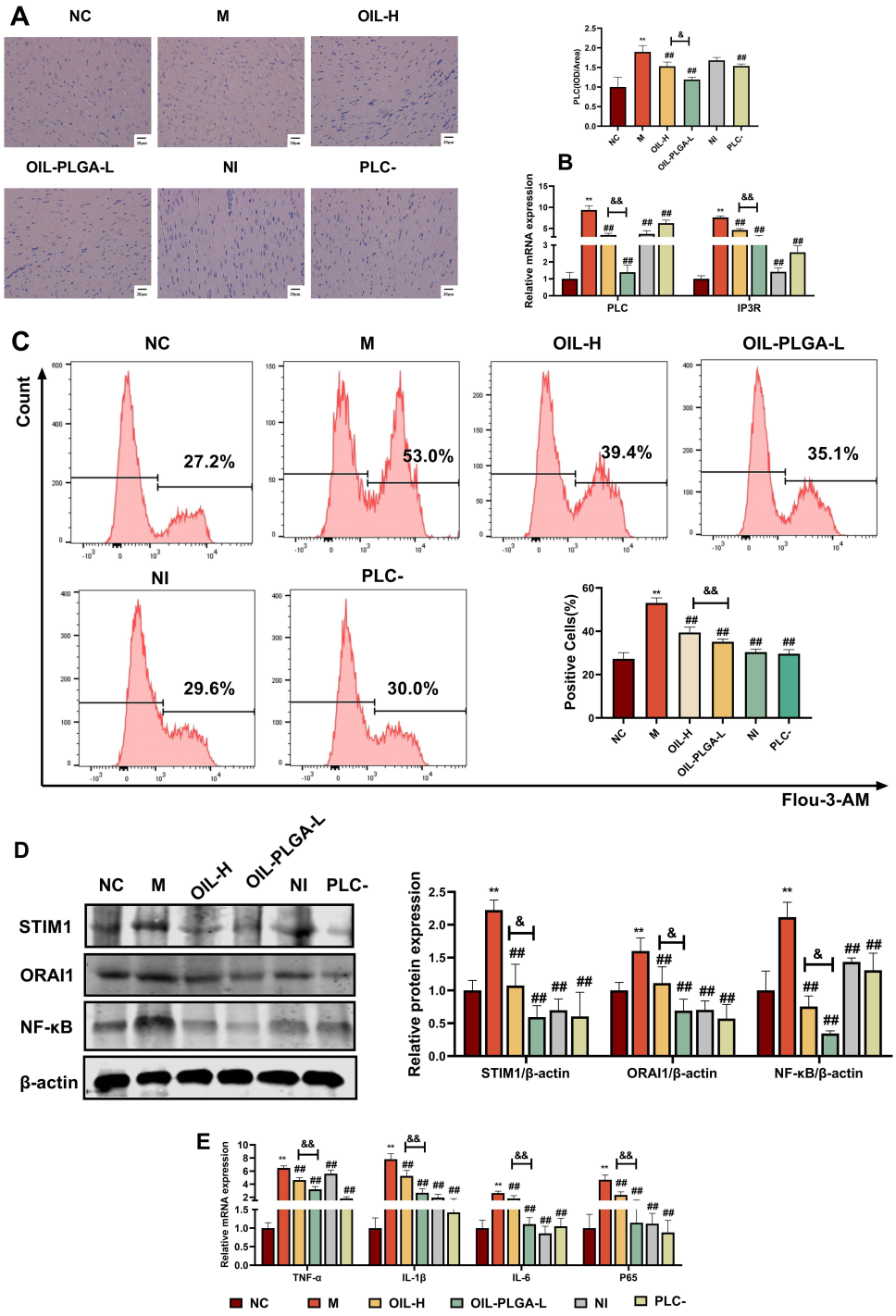

Figure 6 Effects of OIL-NPs on PLC/IP3R/Ca^{2+} signaling pathway in myocardial tissue of PH rats. (**A**) Effects of OIL-NPs on PLC protein expression in myocardial tissue of PH rats. (**B**) Effects of OIL-NPs on PLC and IP3R mRNA expression in myocardial tissue of PH rats. (**C**) Effects of OIL-NPs on Ca^{2+} content in myocardial tissue of rats with PH. (**D**) Effects of OIL-NPs on the expression of STIM1, ORAI1 and NF-κB proteins in myocardial tissue of rats with PH. (**E**) Effects of OIL-NPs on TNF-α, IL-1β, IL-6 and P65 mRNA expression in myocardial tissue of PH rats.

Notes: Data are the mean ± SD (n = 6). $^{**}P<0.01$ vs the NC group. $^{\#\#}P<0.01$ vs the M group. $^{\&}P<0.05$, $^{\&\&}P<0.01$ vs the OIL-H group.

Abbreviations: NC, control group; M, model group with 60 mg/kg monocrotaline, i.p. OIL-H, 40 mg/kg fatty oil, i.v. OIL-PLGA-L, 20 mg/kg fatty oil-loaded PLGA nanoparticles, i.v. NI, 0.1 mg/kg nifedipine, i.v. PLC-, 20 mg/kg neomycin sulfate, i.v. PLC, primary antibodies against phospholipase C. IP3R, inositol 1,4,5-triphosphate receptor. STIM1, stromal interaction molecule 1. ORAI1, calcium release-activated calcium channel modulator 1. NF-κB, nuclear factor kappaB. TNF-α, tumor necrosis factor-α. IL-1β, interleukin-1β. IL-6, interleukin-6.

negative source markers) (Figure 7G and Table 2). The metabolic pathways significantly affected by these differential metabolites mainly include linoleic acid metabolism, taurine and hypotaurine metabolism, glycerophospholipid metabolism, phosphatidylinositol signaling system, etc. (Figure 7H). The cluster heat map analysis of these metabolites is shown in the Figure 7I. In order to further verify the correlation between the above experimental biochemical indicators and serum metabolomics results, we analyzed the correlation between the key metabolites and PLC/IP3R/Ca^{2+} signaling pathway and related inflammatory factors. The results showed that the related indicators of Ca^{2+} signaling pathway were closely related to linoleic acid, myo-inositol, taurine, LysoPC, LysoPA and other markers (Figure 7J). This suggests that OIL-NPs may play a role in anti-pulmonary hypertension by improving related biomarkers through PLC/IP3R/Ca^{2+} signaling pathway. Finally, we constructed a network map of possible metabolic pathways for the differential metabolites (Figure 7K).

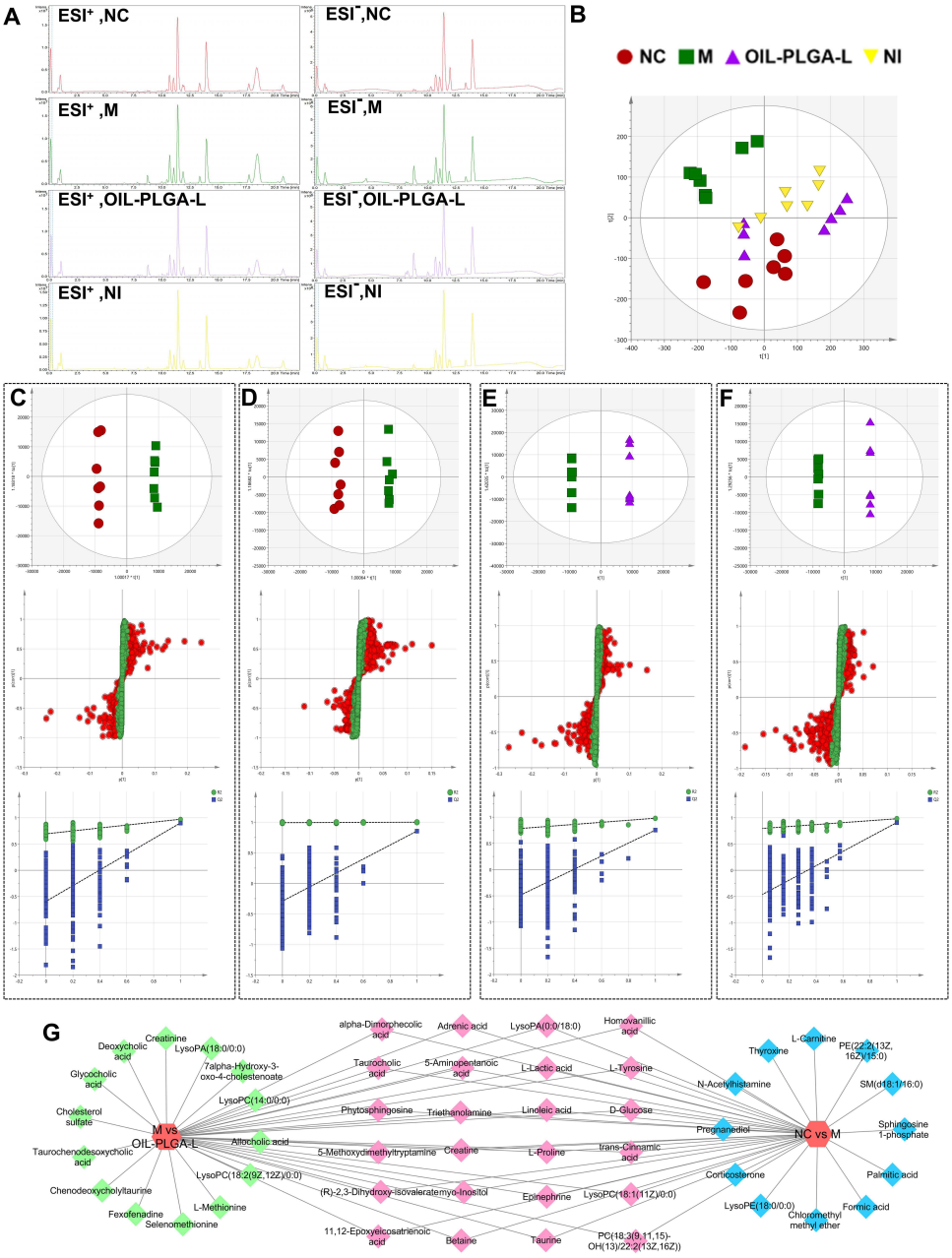

Figure 7 Continued.

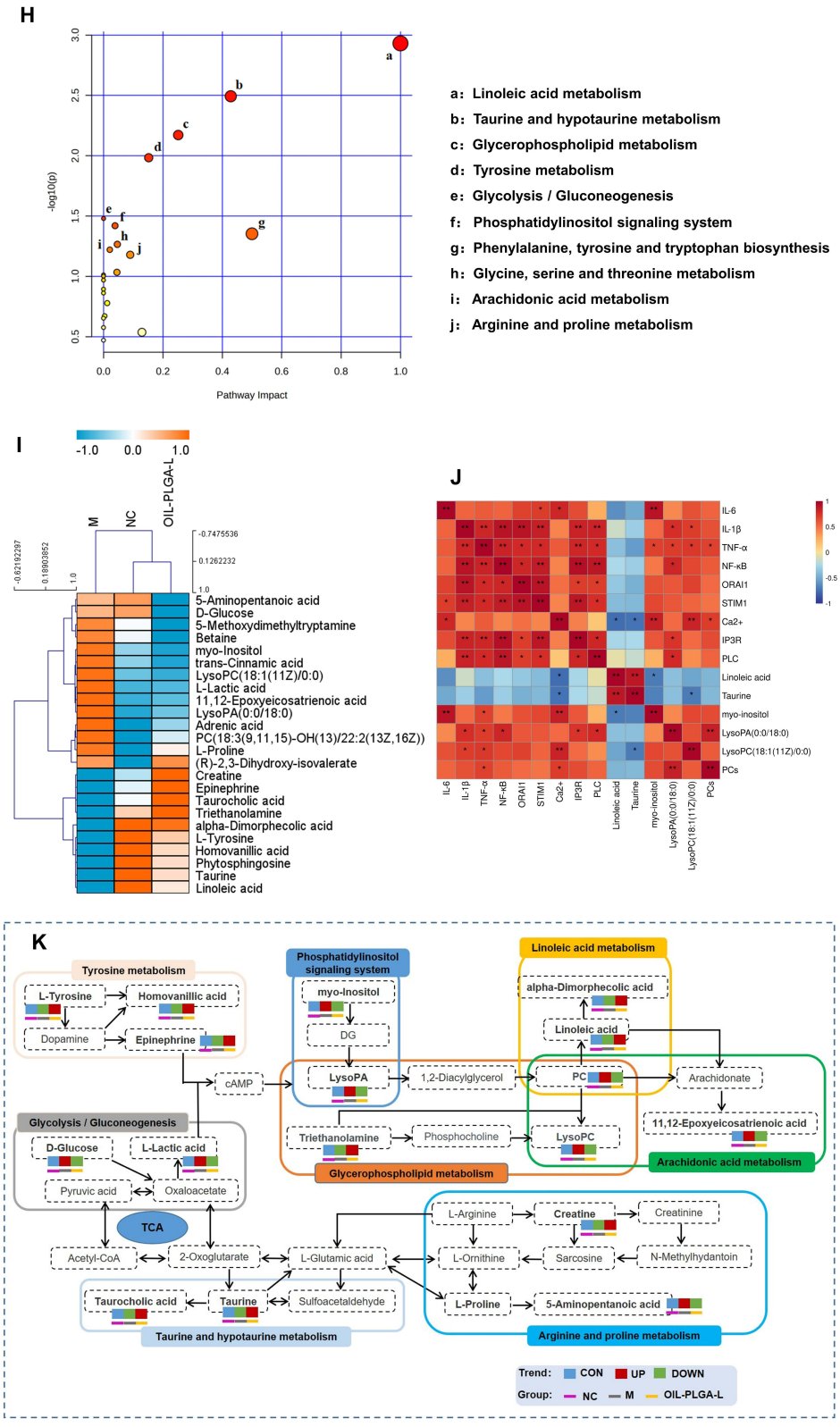

Figure 7 Metabolic serum profiling. (**A**) Base peak chromatogram of NC group, M group, OIL-PLGA-L group and NI group. (**B**) PCA scores of NC group, M group, OIL-PLGA-L group and NI group (R^2=0.352, Q^2=0.167). (**C**) OPLS-DA score scatter plot, S-plot and validation plot of NC group and M group (ESI^+, R^2X=0.739, R^2Y=0.998, Q^2=0.778). (**D**) OPLS-DA score scatter plot, S-plot and validation plot of NC group and M group (ESI^-, R^2X=0.471, R^2Y=0.995, Q^2=0.863). (**E**) OPLS-DA score scatter plot, S-plot and validation plot of M group and OIL-PLGA-L group (ESI^+, R^2X=0.87, R^2Y=1, Q^2=0.81). (**F**) OPLS-DA score scatter plot, S-plot and validation plot of M group and OIL-PLGA-L group (ESI^-, R^2X=0.786, R^2Y=1, Q^2=0.872). (**G**) Network diagram of all differential metabolites. (**H**) Diagram of metabolic pathway analysis. (**I**) Cluster heat map analysis. (**J**) Correlation analysis (*P<0.05; **P<0.01). (**K**) Graph of the metabolic network for PH treated with OIL-NPs.

Table 2 Analysis of 24 Differential Markers

No.	Metabolite	RT/min	MW	Adduct	Formula	Source Mode
1	L-Proline	1.0	116.0706	M+H	$C_5H_9NO_2$	ESI^+
2	5-Aminopentanoic acid	1.0	118.0862	M+H	$C_5H_{11}NO_2$	ESI^+
3	Triethanolamine	1.2	132.1019	M+H-H_2O	$C_6H_{15}NO_3$	ESI^+
4	Creatine	1.2	132.0766	M+H	$C_4H_9N_3O_2$	ESI^+
5	Betaine	1.0	140.0683	M+Na	$C_5H_{12}NO_2$	ESI^+
6	Homovanillic acid	1.2	165.0544	M+H-H_2O	$C_9H_{10}O_4$	ESI^+
7	Epinephrine	1.2	166.0864	M+H-H_2O	$C_9H_{13}NO_3$	ESI^+
8	L-Tyrosine	1.0	182.081	M+H	$C_9H_{11}NO_3$	ESI^+
9	D-Glucose	1.0	203.0529	M+Na	$C_6H_{12}O_6$	ESI^+
10	Linoleic acid	12.0	303.2303	M+Na	$C_{18}H_{32}O_2$	ESI^+
11	Phytosphingosine	11.8	318.2987	M+H	$C_{18}H_{39}NO_3$	ESI^+
12	Adrenic acid	8.8	355.2617	M+Na	$C_{22}H_{36}O_2$	ESI^+
13	LysoPA(0:0/18:0)	8.8	507.2694	M+H+HCOONa	$C_{21}H_{43}O_7P$	ESI^+
14	LysoPC(18:1(11Z)/0:0)	10.8	544.3379	M+Na	$C_{26}H_{52}NO_7P$	ESI^+
15	PC(18:3(9,11,15)-OH(13)/22:2(13Z,16Z))	8.8	834.6047	M+H-H_2O	$C_{48}H_{86}NO_9P$	ESI^+
16	Taurine	1.0	124.0073	M-H	$C_2H_7NO_3S$	ESI^-
17	L-Lactic acid	1.0	179.056	2M-H	$C_3H_6O_3$	ESI^-
18	(R)-2,3-Dihydroxy-isovalerate	1.0	201.0382	M-H+HCOONa	$C_5H_{10}O_4$	ESI^-
19	Trans-Cinnamic acid	1.0	215.033	M-H+HCOONa	$C_9H_8O_2$	ESI^-
20	Myo-Inositol	1.0	225.0618	M+Na	$C_6H_{12}O_6$	ESI^-
21	Alpha-Dimorphecolic acid	11.4	295.2291	M-H	$C_{18}H_{32}O_3$	ESI^-
22	11,12-Epoxyeicosatrienoic acid	12.0	387.2169	M-H+HCOONa	$C_{20}H_{32}O_3$	ESI^-
23	5-Methoxydimethyltryptamine	9.2	435.2768	2M-H	$C_{13}H_{18}N_2O$	ESI^-
24	Taurocholic acid	7.0	514.2857	M-H	$C_{26}H_{45}NO_7S$	ESI^-

Discussion

As a traditional Chinese medicine, *Descurainia sophia* has significant curative effect in treating lung diseases and heart failure.[11,20] Early laboratory research found that the fatty oil component in *Descurainia sophia* is one of the active components, so the experiment wanted to explore whether the fatty oil has anti-PH effect. However, the fatty oil component has poor solubility, low bioavailability and instability, so we prepared OIL-NPs. PLGA is a biodegradable polymer with good biocompatibility. It can be degraded into lactic acid and glycolic acid in human body. Due to its good biocompatibility and safety, PLGA is widely used as a carrier of various nano preparations.[41,42] Polyethylene glycol (PEG) is the most commonly used hydrophilic compound with nano surface modification and has good biocompatibility. PEG is introduced to the surface of hydrophobic PLGA polymer as a hydrophilic component to form PEG-PLGA copolymer, which can effectively improve the water solubility of the carrier and increase the stability of the drug.[43] Therefore, PEG-PLGA copolymer was selected as the carrier in this experiment to build a fatty oil nanoparticles co-

delivery system. The final prepared OIL-NPs were uniformly dispersed with an average particle size of 323.87 ± 4.81 nm, PDI was 0.157 ± 0.009, the encapsulation rate was 60.09% ± 0.55%, with good dispersion and stability.

Pulmonary hypertension (PH) is a pulmonary vascular disease characterized by progressive elevation of pulmonary artery pressure. With the continuous increase of pulmonary vascular resistance, the patient's right heart load increases, right heart failure occurs, and ultimately leads to death.[5] At present, there is no specific drug for pulmonary hypertension and it cannot be cured. Therefore, actively exploring drugs for prevention and treatment of pulmonary hypertension has become an urgent problem to be solved.[44] Previous studies have shown that abnormal proliferation of RPASMC cells is the main cause of PH[45,46] and abnormal mitochondrial fission and fusion is closely related to abnormal proliferation of RPASMC cells.[47] Mitochondrial fission and fusion is mainly regulated by the mitochondrial dynein protein Drp1 and the mitochondrial fusion-related protein MFN2. MFN2 is located in the mitochondrial outer membrane, which can promote the fusion of two adjacent mitochondria and repair mitochondrial damage. Drp1 can promote the division of mitochondria and is conducive to cell proliferation.[48,49] Studies have shown that increasing MFN2 and decreasing Drp1 expression will increase mitochondrial membrane permeability and decrease mitochondrial membrane potential, which in turn activates the caspase family, reduces Bcl-2 expression and increases Bax expression, triggering mitochondria-mediated cellular endogenous apoptotic pathway and promoting apoptosis.[25,50] In order to explore the effect of OIL-NPs on RPASMC cells, this experiment established a malignant proliferation model of RPASMC cells by hypoxia chamber induction. We found that OIL and OIL-NPs can inhibit the PLC/IP3R/Ca^{2+} signal pathway, reduce the mitochondrial membrane potential and Drp1 of RPASMC cells, increase the expression of MFN2, and promote the apoptosis of RPASMC cells, and the effect of OIL-NPs is better than that of fatty oil. In order to further verify that OIL-NPs play a role by inhibiting PLC, we designed the PLC agonist group for reverse validation, and found that the PLC agonist group has no significant effect. These results suggest that OIL-NPs may promote RPASMC apoptosis by inhibiting PLC/IP3R/Ca2+ signaling pathway.

After initially establishing the role of OIL-NPs in cells in vitro, in vivo experiments in rats were performed in the present study. At present, the commonly accepted method of pulmonary hypertension rat model is intraperitoneal injection of monocrotaline (60 mg/kg). The toxic metabolite produced by monocrotaline metabolized by rat liver P450 enzyme system specifically damages pulmonary vascular endothelial cells, resulting in increased secretion of inflammatory factors such as TNF-α, IL-6 and IL-1β[51,52] and imbalance of vasoactive substance NO/ET-1, which mediates proliferation of pulmonary artery smooth muscle cells. Eventually, it causes pulmonary hypertension and right heart failure.[20,53] Right heart hypertrophy index, pulmonary artery pressure, cardiopulmonary pathological injury and function are vital indicators to evaluate the effect of pulmonary hypertension model.[53] The experiment found that in M group, the pulmonary artery pressure and right heart hypertrophy index were increased, pulmonary vascular wall thickened, myocardial cell hypertrophy damaged, cardiac function decreased, the level of inflammatory factor TNF-α was increased, and the level of NO/ET-1 was unbalanced. Neomycin sulfate is a known PLC inhibitor, which is widely used to inhibit PLC expression in PLC-related experimental studies.[54] In the experiment, fatty oil, OIL-NPs and PLC inhibitors could reverse the pathological damage, reduce pulmonary artery pressure, and improve heart and lung tissue damage in rats, and the OIL-PLGA-L group was better than the OIL-H group. Therefore, OIL-NPs may exert an anti-pH effect by inhibiting PLC.

PLC/IP3R/Ca^{2+} signaling pathway plays an important role in cell proliferation and apoptosis,[55,56] vascular contraction and relaxation,[57] and mitochondrial function.[58,59] Phospholipase PLC is expressed in the cell membrane and is a key enzyme in signal transduction. Activated PLC catalyzes PIR2 to produce IP3 and DAG. IP3 can bind to inositol triphosphate receptor (IP3R) on the endoplasmic reticulum. IP3R is a Ca^{2+} release channel in the endoplasmic reticulum, and activation of IP3R can trigger the massive release of Ca^{2+} from the endoplasmic reticulum into the cytoplasm, resulting in Ca^{2+} overload in the cytoplasm and Ca^{2+} depletion in the endoplasmic reticulum.[60,61] The endoplasmic reticulum (ER) is the main organelle for intracellular Ca^{2+} storage, and the depletion of Ca^{2+} in the ER can activate store-operated calcium channels (SOCC).[62] Studies have shown that ORAI1 and STIM1 are important mediators leading to the occurrence of SOCE. ORAI1 is a transmembrane protein involved in the formation of SOCC, and STIM1 is a Ca^{2+} sensor located near the Ca^{2+} storage area and can transmit Ca^{2+} storage information to the cell membrane. ORAI1 and STIM1 expression is increased upon Ca^{2+} depletion in the ER.[63,64] Recent studies have found abnormal activation of PLC/IP3R/Ca^{2+} signaling,[12,65] resulting in abnormal opening of SOCC mediated by ORAI1 and STIM1, which may be related to the development of pulmonary hypertension.[66] The results showed that fatty oil, OIL-NPs and PLC inhibitor could inhibit PLC/IP3R/Ca^{2+} signaling pathway, reduce Ca^{2+} content and ORAI1 and STIM1 protein expression in heart and

lung tissues of rats, and the effect of OIL-NPs was better than that of fatty oil. These results suggest that OIL-NPs may play an anti-pH role by inhibiting the expression of PLC/IP3R/Ca^{2+} signaling pathway to alleviate SOCE and reduce intracellular Ca^{2+} content. Previous studies have shown that intracellular calcium overload can increase the expression of NF-κB.[67,68] NF-κB is a nuclear transcription factor, and its excessive activation is closely related to cell proliferation and increased expression of inflammatory factors.[69,70] The results showed that fatty oil, OIL-NPs and PLC inhibitor could reduce the expression of NF-κB and the mRNA expression levels of TNF-α, IL-6 and IL-1β, and the effect of OIL-NPs was better than that of fatty oil. This further suggests that OIL-NPs may play an anti-PH role by inhibiting the PLC/IP3R/Ca^{2+} signaling pathway.

In order to study the metabolic processes involved in the intervention of fatty oil components in pulmonary hypertension, the method of metabolomics was used in this experiment, and a total of 24 biomarkers were screened out. These metabolites were mainly involved in linoleic acid metabolism, taurine and hypotaurine metabolism, glycerophospholipid metabolism, phosphatidylinositol signaling system and other metabolic processes. In linoleic acid metabolism, we detected a decrease in linoleic acid content in the model group, and after administration, linoleic acid content increased. Studies have shown that linoleic acid has anti-thrombotic and anti-proliferation effects, and further studies have shown that linoleic acid can inhibit the expression of PLC,[71] thereby reducing Ca^{2+} release. In taurine and hypotaurine metabolism, we detected 2 major markers, taurine and taurocholic acid. Taurine is one of the most abundant amino acids in most animal tissues, and our results showed that taurine content was up-regulated after administration of OIL-NPs. Studies have shown that taurine has anti-inflammatory, anti-oxidation, and immunomodulatory effects,[72] and some studies have shown that taurine can down-regulate Ca^{2+} release through the PLC/IP3 signaling pathway.[73] Meanwhile, metabolic disorder of phosphatidylinositol signaling system was also detected. Inositol is catalyzed by phosphatidylinositol synthetase to form phosphatidylinositol (PI). Under the catalysis of phosphatidylinositol kinase, PI forms different forms of phosphatidylinositol, such as PIP2 and PIP3.[74] The main function of PLC is to catalyze PIP2 to produce inositol triphosphate (IP3) and DAG, and IP3 acts on IP3R to promote the release of Ca^{2+}. Therefore, the increase in inositol content will indirectly promote the release of Ca^{2+}. Our experimental data showed that myo-inositol content increased in the M group, which promoted the release of Ca^{2+}, and decreased after administration. Three major markers, PC, LysoPC and LysoPA, were detected in glycerophospholipid metabolism. It has been shown that PC is metabolized to produce choline, which acts on Sigma-1 receptors in the endoplasmic reticulum to promote the release of Ca^{2+} into the cell.[75] LysoPC activates Transient receptor potential cation channel 6 (TRPC6), thereby promoting the release of Ca^{2+} into cells.[76] Our assay results showed that after drug administration, PC, LysoPC content decreased, which in turn reduced Ca^{2+} release into the cells. In summary, the metabolomic results also suggested that OIL-NPs might exert their anti-pulmonary hypertension effects by inhibiting PLC/IP3R/Ca^{2+} signaling pathway.

Conclusion

OIL-NPs not only exhibit beneficial effects but also do not appear to have significant biological toxicity, indicating their enormous potential as candidate methods for treating pulmonary hypertension. The anti-pH effect of OIL-NPs may be related to the inhibition of PLC/IP3R/Ca^{2+} signaling pathway. This study provides a preliminary basis for OIL-NPs to reduce pulmonary hypertension. Nonetheless, the deeper mechanisms need to be further investigated.

Acknowledgment

This work was supported by the National Key Research and Development Program (Major Project for Research of the Modernization of TCM; 2019YFC1708802), Henan Province High-Level Personnel Special Support ("ZhongYuan One Thousand People Plan"; Zhongyuan Leading Talent (ZYQR201810080)) and Key Scientific Research Projects of Colleges and Universities of Henan Province (21A360014).

Author Contributions

All authors made a significant contribution to the work reported, whether that is in the conception, study design, execution, acquisition of data, analysis and interpretation, or in all these areas; took part in drafting, revising or critically reviewing the article; gave final approval of the version to be published; have agreed on the journal to which the article has been submitted; and agree to be accountable for all aspects of the work.

Disclosure

The authors declare no conflicts of interest.

References

1. Barberà JA, Román A, Gómez-Sánchez M, et al. Guidelines on the diagnosis and treatment of pulmonary hypertension: summary of recommendations. *Archivos de bronconeumologia*. 2018;54(4):205–215. doi:10.1016/j.arbr.2017.11.017
2. Beshay S, Sahay S, Humbert M. Evaluation and management of pulmonary arterial hypertension. *Respir Med*. 2020;171:106099. doi:10.1016/j.rmed.2020.106099
3. Ramirez RL, Pienkos SM, de Jesus Perez V, Zamanian RT. Pulmonary arterial hypertension secondary to drugs and toxins. *Clinics Chest Med*. 2021;42(1):19–38. doi:10.1016/j.ccm.2020.11.008
4. Shah AJ, Vorla M, Kalra DK. Molecular pathways in pulmonary arterial hypertension. *Int J Mol Sci*. 2022;23(17):10001. doi:10.3390/ijms231710001
5. Huang WC, Hsu CH, Sung SH, et al. 2018 TSOC guideline focused update on diagnosis and treatment of pulmonary arterial hypertension. *J Formos Med Assoc*. 2019;118(12):1584–1609. doi:10.1016/j.jfma.2018.12.009
6. Rajagopal S, Yu YA. The pathobiology of pulmonary arterial hypertension. *Cardiol Clinics*. 2022;40(1):1–12. doi:10.1016/j.ccl.2021.08.001
7. Thompson AAR, Lawrie A. Targeting vascular remodeling to treat pulmonary arterial hypertension. *Trends Mol Med*. 2017;23(1):31–45. doi:10.1016/j.molmed.2016.11.005
8. Robinson JC, Pugliese SC, Fox DL, Badesch DB. Anticoagulation in pulmonary arterial hypertension. *Curr Hypertens Rep*. 2016;18(6):47. doi:10.1007/s11906-016-0657-2
9. Ma B, Cao Y, Qin J, Chen Z, Hu G, Li Q. Pulmonary artery smooth muscle cell phenotypic switching: a key event in the early stage of pulmonary artery hypertension. *Drug Discovery Today*. 2023;28(5):103559. doi:10.1016/j.drudis.2023.103559
10. Zhang C, Sun Y, Guo Y, Xu J, Zhao H. JMJD1C promotes smooth muscle cell proliferation by activating glycolysis in pulmonary arterial hypertension. *Cell Death Discovery*. 2023;9(1):98. doi:10.1038/s41420-023-01390-5
11. Xu J, Zhong Y, Yin H, et al. Methylation-mediated silencing of PTPRD induces pulmonary hypertension by promoting pulmonary arterial smooth muscle cell migration via the PDGFRB/PLCγ1 axis. *J Hypertens*. 2022;40(9):1795–1807. doi:10.1097/HJH.0000000000003220
12. Masson B, Montani D, Humbert M, Capuano V, Antigny F. Role of store-operated Ca(2+) entry in the pulmonary vascular remodeling occurring in pulmonary arterial hypertension. *Biomolecules*. 2021;11(12):1781. doi:10.3390/biom11121781
13. Huang Y, Lei C, Xie W, et al. Oxidation of ryanodine receptors promotes Ca(2+) leakage and contributes to right ventricular dysfunction in pulmonary hypertension. *Hypertension*. 2021;77(1):59–71. doi:10.1161/HYPERTENSIONAHA.120.15561
14. Deng L, Chen J, Chen B, et al. LncPTSR triggers vascular remodeling in pulmonary hypertension by regulating [Ca(2+)](i) in pulmonary arterial smooth muscle cells. *Am J Respir Cell Mol Biol*. 2022;66(5):524–538. doi:10.1165/rcmb.2020-0480OC
15. Kanemaru K, Nakamura Y. Activation mechanisms and diverse functions of mammalian phospholipase C. *Biomolecules*. 2023;13(6):915. doi:10.3390/biom13060915
16. Yamamura A, Ohara N, Tsukamoto K, Su Y. Inhibition of excessive cell proliferation by calcilytics in idiopathic pulmonary arterial hypertension. *PLoS One*. 2015;10(9):e0138384. doi:10.1371/journal.pone.0138384
17. Liu B, Zhu L, Yuan P, et al. Comprehensive identification of signaling pathways for idiopathic pulmonary arterial hypertension. *Am J Physiol Cell Physiol*. 2020;318(5):C913–C930. doi:10.1152/ajpcell.00382.2019
18. Baek SJ, Chun JM, Kang TW, et al. Identification of epigenetic mechanisms involved in the anti-asthmatic effects of descurainia sophia seed extract based on a multi-omics approach. *Molecules*. 2018;23(11):2879. doi:10.3390/molecules23112879
19. Zhang J, Zhou N, Wang Y, et al. Protective effects of Descurainia sophia seeds extract and its fractions on pulmonary edema by untargeted urine and serum metabolomics strategy. *Front Pharmacol*. 2023;14:1080962. doi:10.3389/fphar.2023.1080962
20. Kim SB, Seo YS, Kim HS, et al. Anti-asthmatic effects of lepidii seu Descurainiae Semen plant species in ovalbumin-induced asthmatic mice. *J Ethnopharmacol*. 2019;244:112083. doi:10.1016/j.jep.2019.112083
21. Hsieh PC, Kuo CY, Lee YH, et al. Therapeutic effects and mechanisms of actions of Descurainia sophia. *Int J Med Sci*. 2020;17(14):2163–2170. doi:10.7150/ijms.47357
22. Ruan Y, Yuan PP, Li PY, et al. Tingli Dazao Xiefei Decoction ameliorates asthma in vivo and in vitro from lung to intestine by modifying NO-CO metabolic disorder mediated inflammation, immune imbalance, cellular barrier damage, oxidative stress and intestinal bacterial disorders. *J Ethnopharmacol*. 2023;313:116503. doi:10.1016/j.jep.2023.116503
23. Fu Y, Yuan P, Hou Y, et al. Difference of the upfloater ephedrae herba and the downsinker descurainiae semen lepidii semen on asthma based on the GnRHR signaling pathway. *J Tradit Chin Med*. 2022;37(05):2553–2562.
24. Rice TW, Wheeler AP, Thompson BT, deBoisblanc BP, Steingrub J, Rock P. Enteral omega-3 fatty acid, gamma-linolenic acid, and antioxidant supplementation in acute lung injury. *JAMA*. 2011;306(14):1574–1581. doi:10.1001/jama.2011.1435
25. Zhu X, Wang B, Zhang X, et al. Alpha-linolenic acid protects against lipopolysaccharide-induced acute lung injury through anti-inflammatory and anti-oxidative pathways. *Microb Pathogenesis*. 2020;142:104077. doi:10.1016/j.micpath.2020.104077
26. Benoit B, Bruno J, Kayal F, et al. Saturated and unsaturated fatty acids differently modulate colonic goblet cells in vitro and in rat pups. *J Nutr*. 2015;145(8):1754–1762. doi:10.3945/jn.115.211441
27. Chander A, Fisher AB. Choline-phosphate cytidyltransferase activity and phosphatidylcholine synthesis in rat granular pneumocytes are increased with exogenous fatty acids. *BBA*. 1988;958(3):343–351. doi:10.1016/0005-2760(88)90219-6
28. Ahrari A, Najafzadehvarzi H, Taravati A, Tohidi F. The inhibitory effect of PLGA-encapsulated berberine on hepatotoxicity and α-smooth muscle actin (α-SMA) gene expression. *Life Sci*. 2021;284:119884. doi:10.1016/j.lfs.2021.119884
29. Wan S, Zhang L, Quan Y, Wei K. Resveratrol-loaded PLGA nanoparticles: enhanced stability, solubility and bioactivity of resveratrol for non-alcoholic fatty liver disease therapy. *Royal Soc Open Sci*. 2018;5(11):181457. doi:10.1098/rsos.181457
30. Xu R, Wang J, Xu J, et al. Rhynchophylline loaded-mPEG-PLGA nanoparticles coated with tween-80 for preliminary study in Alzheimer's disease. *Int J Nanomed*. 2020;15:1149–1160. doi:10.2147/IJN.S236922

31. Sun Y, Wan W, Zhao X, et al. Chronic Sigma 1 receptor activation alleviates right ventricular dysfunction secondary to pulmonary arterial hypertension. *Bioengineered*. 2022;13(4):10843–10856. doi:10.1080/21655979.2022.2065953
32. Zhou N, Li Z, Wang JJ, et al. Correlation analysis between extracts and endogenous metabolites to characterise the influence of salt-processing on compatibility mechanism of "Psoraleae Fructus & Foeniculi Fructus". *J Ethnopharmacol*. 2021;270:113782. doi:10.1016/j.jep.2021.113782
33. Gong JH, Zhang YL, He JL, et al. Extractions of oil from Descurainia sophia seed using supercritical CO2, chemical compositions by GC-MS and evaluation of the anti-tussive, expectorant and anti-asthmatic activities. *Molecules*. 2015;20(7):13296–13312. doi:10.3390/molecules200713296
34. Boskabady MH, Kaveh M, Shakeri F, Mohammadian Roshan N, Rezaee R. Alpha-linolenic acid ameliorates bronchial asthma features in ovalbumin-sensitized rats. *J Pharm Pharmacol*. 2019;71(7):1089–1099. doi:10.1111/jphp.13094
35. Kim YJ, Lee KP, Lee DY, Kim YT, Baek S, Yoon MS. Inhibitory effect of modified silkworm pupae oil in PDGF-BB-induced proliferation and migration of vascular smooth muscle cells. *Food Sci Biotechnol*. 2020;29(8):1091–1099. doi:10.1007/s10068-020-00742-6
36. de Oliveira AP, Franco Ede S, Rodrigues Barreto R, et al. Effect of semisolid formulation of Persea americana Mill (avocado) oil on wound healing in rats. *Evid Based Complement Alternat Med*. 2013;2013:472382. doi:10.1155/2013/472382
37. Hamdi A, Majouli K, Abdelhamid A, et al. Pharmacological activities of the organic extracts and fatty acid composition of the petroleum ether extract from Haplophyllum tuberculatum leaves. *J Ethnopharmacol*. 2018;216:97–103. doi:10.1016/j.jep.2018.01.012
38. Murru E, Lopes PA, Carta G, et al. Different dietary N-3 polyunsaturated fatty acid formulations distinctively modify tissue fatty acid and n-acylethanolamine profiles. *Nutrients*. 2021;13(2):625. doi:10.3390/nu13020625
39. Chen H, Zheng Y, Tian G, et al. Oral delivery of DMAB-modified docetaxel-loaded PLGA-TPGS nanoparticles for cancer chemotherapy. *Nanoscale Res Lett*. 2011;6(1):4. doi:10.1007/s11671-010-9741-8
40. Fu Y, Yuan P, Zheng Y, et al. Pseudoephedrine nanoparticles alleviate adriamycin-induced reproductive toxicity through the GnRhR signaling pathway. *Int J Nanomed*. 2022;17:1549–1566. doi:10.2147/IJN.S348673
41. Rocha CV, Gonçalves V, da Silva MC, Bañobre-López M, Gallo J. PLGA-based composites for various biomedical applications. *Int J Mol Sci*. 2022;23(4):2034. doi:10.3390/ijms23042034
42. Mahar R, Chakraborty A, Nainwal N, Bahuguna R, Sajwan M, Jakhmola V. Application of PLGA as a biodegradable and biocompatible polymer for pulmonary delivery of drugs. *AAPS Pharm Sci Tech*. 2023;24(1):39. doi:10.1208/s12249-023-02502-1
43. Zhang LL, Wang J, Wang J, et al. Drug-loaded PEG-PLGA nanoparticles for cancer treatment. *Front Pharmacol*. 2022;13:990505. doi:10.3389/fphar.2022.990505
44. Galiè N, Channick RN, Frantz RP, et al. Risk stratification and medical therapy of pulmonary arterial hypertension. *Europ resp J*. 2019;53(1):1801889. doi:10.1183/13993003.01889-2018
45. Chen YJ, Li Y, Guo X, et al. Upregulation of IRF9 contributes to pulmonary artery smooth muscle cell proliferation during pulmonary arterial hypertension. *Front Pharmacol*. 2021;12:773235. doi:10.3389/fphar.2021.773235
46. Hu S, Zhao Y, Qiu C, Li Y. RAS protein activator like 2 promotes the proliferation and migration of pulmonary artery smooth muscle cell through AKT/mammalian target of Rapamycin complex 1 pathway in pulmonary hypertension. *Bioengineered*. 2022;13(2):3516–3526. doi:10.1080/21655979.2021.1997879
47. Xiao F, Zhang R, Wang L. Inhibitors of mitochondrial dynamics mediated by dynamin-related protein 1 in pulmonary arterial hypertension. *Front Cell Dev Biol*. 2022;10:913904. doi:10.3389/fcell.2022.913904
48. Ryan J, Dasgupta A, Huston J, Chen KH, Archer SL. Mitochondrial dynamics in pulmonary arterial hypertension. *J Mol Med*. 2015;93(3):229–242. doi:10.1007/s00109-015-1263-5
49. Uchikado Y, Ikeda Y, Ohishi M. Current understanding of the pivotal role of mitochondrial dynamics in cardiovascular diseases and senescence. *Front Cardiovasc Med*. 2022;9:905072. doi:10.3389/fcvm.2022.905072
50. Parra V, Bravo-Sagua R, Norambuena-Soto I, et al. Inhibition of mitochondrial fission prevents hypoxia-induced metabolic shift and cellular proliferation of pulmonary arterial smooth muscle cells. *Biochim Biophys Acta Mol Basis Dis*. 2017;1863(11):2891–2903. doi:10.1016/j.bbadis.2017.07.018
51. Tang C, Luo Y, Li S, Huang B, Xu S, Li L. Characteristics of inflammation process in monocrotaline-induced pulmonary arterial hypertension in rats. *Biomed Pharmacother*. 2021;133:111081. doi:10.1016/j.biopha.2020.111081
52. Krzyżewska A, Baranowska-Kuczko M, Jastrząb A, Kasacka I, Kozłowska H. Cannabidiol improves antioxidant capacity and reduces inflammation in the lungs of rats with monocrotaline-induced pulmonary hypertension. *Molecules*. 2022;27(10):3327. doi:10.3390/molecules27103327
53. Dignam JP, Scott TE, Kemp-Harper BK, Hobbs AJ. Animal models of pulmonary hypertension: getting to the heart of the problem. *Br J Pharmacol*. 2022;179(5):811–837. doi:10.1111/bph.15444
54. Suzuki T, Imai J, Yamada T, et al. Interleukin-6 enhances glucose-stimulated insulin secretion from pancreatic beta-cells: potential involvement of the PLC-IP3-dependent pathway. *Diabetes*. 2011;60(2):537–547. doi:10.2337/db10-0796
55. Gao T, Yang P, Fu D, et al. The protective effect of allicin on myocardial ischemia-reperfusion by inhibition of Ca(2+) overload-induced cardiomyocyte apoptosis via the PI3K/GRK2/PLC-γ/IP3R signaling pathway. *Aging*. 2021;13(15):19643–19656. doi:10.18632/aging.203375
56. Wang S, Li C, Sun P, et al. PCV2 triggers PK-15 cell apoptosis through the PLC-IP3R-Ca(2+) signaling pathway. *Front Microbiol*. 2021;12:674907. doi:10.3389/fmicb.2021.674907
57. Potje SR, Isbatan A, Tostes RC, et al. Glypican 1 and syndecan 1 differently regulate noradrenergic hypertension development: focus on IP3R and calcium. *Pharmacol Res*. 2021;172:105813. doi:10.1016/j.phrs.2021.105813
58. Ye L, Zeng Q, Ling M, et al. Inhibition of IP3R/Ca2+ dysregulation protects mice from ventilator-induced lung injury via endoplasmic reticulum and mitochondrial pathways. *Front Immunol*. 2021;12:729094. doi:10.3389/fimmu.2021.729094
59. Wong CO, Karagas NE, Jung J, et al. Regulation of longevity by depolarization-induced activation of PLC-β-IP(3)R signaling in neurons. *Proc Natl Acad Sci U S A*. 2021;118(16). doi:10.1073/pnas.2004253118
60. Souza Bomfim GH, Mitaishvili E, Aguiar TF, Lacruz RS. Mibefradil alters intracellular calcium concentration by activation of phospholipase C and IP(3) receptor function. *Mol Biomed*. 2021;2(1):12. doi:10.1186/s43556-021-00037-0
61. Ryglewski S, Pflueger HJ, Duch C, Spitzer NC. Expanding the neuron's calcium signaling repertoire: intracellular calcium release via voltage-induced PLC and IP3R activation. *PLoS Biol*. 2007;5(4):e66. doi:10.1371/journal.pbio.0050066
62. Sampieri A, Santoyo K, Asanov A, Vaca L. Association of the IP3R to STIM1 provides a reduced intraluminal calcium microenvironment, resulting in enhanced store-operated calcium entry. *Sci Rep*. 2018;8(1):13252. doi:10.1038/s41598-018-31621-0

63. Ambudkar IS, de Souza LB, Ong HL. TRPC1, Orai1, and STIM1 in SOCE: friends in tight spaces. *Cell Calcium*. 2017;63:33–39. doi:10.1016/j.ceca.2016.12.009
64. Silva-Rojas R, Laporte J, Böhm J. STIM1/ORAI1 loss-of-function and gain-of-function mutations inversely impact on SOCE and calcium homeostasis and cause multi-systemic mirror diseases. *Front Physiol*. 2020;11:604941. doi:10.3389/fphys.2020.604941
65. Shibata A, Uchida K, Kodo K, et al. Type 2 inositol 1,4,5-trisphosphate receptor inhibits the progression of pulmonary arterial hypertension via calcium signaling and apoptosis. *Heart Vessels*. 2019;34(4):724–734. doi:10.1007/s00380-018-1304-4
66. Sabourin J, Boet A, Rucker-Martin C, et al. Ca(2+) handling remodeling and STIM1L/Orai1/TRPC1/TRPC4 upregulation in monocrotaline-induced right ventricular hypertrophy. *J Mol Cell Cardiol*. 2018;118:208–224. doi:10.1016/j.yjmcc.2018.04.003
67. Davies MJ, Miranda E, Roussel BD, Kaufman RJ, Marciniak SJ, Lomas DA. Neuroserpin polymers activate NF-kappaB by a calcium signaling pathway that is independent of the unfolded protein response. *J Biol Chem*. 2009;284(27):18202–18209. doi:10.1074/jbc.M109.010744
68. Zhang Y, Yang G, Huang S, et al. Regulation of Cr(VI)-Induced premature senescence in L02 hepatocytes by ROS-Ca(2+)-NF-κB signaling. *Oxid Med Cell Longev*. 2022;2022:7295224. doi:10.1155/2022/7295224
69. Jiang R, Tang J, Zhang X, et al. CCN1 promotes inflammation by inducing IL-6 production via α6β1/PI3K/Akt/NF-κB pathway in autoimmune hepatitis. *Front Immunol*. 2022;13:810671. doi:10.3389/fimmu.2022.810671
70. Das R, Mehta DK, Dhanawat M. Medicinal plants in cancer treatment: contribution of Nuclear Factor- Kappa B (NF-kB) Inhibitors. *Mini Rev Med Chem*. 2022;22(15):1938–1962. doi:10.2174/1389557522666220307170126
71. Tao Q, Xiao G, Wang T, et al. Identification of linoleic acid as an antithrombotic component of Wenxin Keli via selective inhibition of p-selectin-mediated platelet activation. *Biomed Pharmacother*. 2022;153:113453. doi:10.1016/j.biopha.2022.113453
72. Zheng J, Qiu G, Zhou Y, Ma K, Cui S. Hepatoprotective effects of taurine against cadmium-induced liver injury in female mice. *Biol Trace Elem Res*. 2023;201(3):1368–1376. doi:10.1007/s12011-022-03252-0
73. Li M, Xi P, Xu Y, et al. Taurine attenuates Streptococcus uberis-induced bovine mammary epithelial cells inflammation via Phosphoinositides/Ca(2+) signaling. *Front Immunol*. 2019;10:1825. doi:10.3389/fimmu.2019.01825
74. Katan M, Cockcroft S, Harwood J, Lloyd-Evans E. Phosphatidylinositol(4,5)bisphosphate: diverse functions at the plasma membrane. *Essays Biochem*. 2020;64(3):513–531. doi:10.1042/EBC20200041
75. Brailoiu E, Chakraborty S, Brailoiu GC, et al. Choline is an intracellular messenger linking extracellular stimuli to IP(3)-Evoked Ca(2+) signals through sigma-1 receptors. *Cell Rep*. 2019;26(2):330–337.e334. doi:10.1016/j.celrep.2018.12.051
76. Putta P, Chaudhuri P, Guardia-Wolff R, Rosenbaum MA, Graham LM. iPLA2 inhibition blocks LysoPC-induced TRPC6 externalization and promotes Re-endothelialization of carotid injuries in hypercholesterolemic mice. *Cell Calcium*. 2023;112:102734. doi:10.1016/j.ceca.2023.102734

International Journal of Nanomedicine Dovepress

Publish your work in this journal

The International Journal of Nanomedicine is an international, peer-reviewed journal focusing on the application of nanotechnology in diagnostics, therapeutics, and drug delivery systems throughout the biomedical field. This journal is indexed on PubMed Central, MedLine, CAS, SciSearch®, Current Contents®/Clinical Medicine, Journal Citation Reports/Science Edition, EMBase, Scopus and the Elsevier Bibliographic databases. The manuscript management system is completely online and includes a very quick and fair peer-review system, which is all easy to use. Visit http://www.dovepress.com/testimonials.php to read real quotes from published authors.

Submit your manuscript here: https://www.dovepress.com/international-journal-of-nanomedicine-journal